Diffusion in Zircon

Daniele J. Cherniak and E. Bruce Watson

Department of Earth and Environmental Sciences
Rensselaer Polytechnic Institute
Troy, New York 12180

INTRODUCTION

Despite its low abundance in most rocks, zircon is extraordinarily useful in interpreting crustal histories. The importance of U-Th-Pb isotopic dating of zircon is well and long established (Davis et al., this volume; Parrish et al., this volume). Zircon also tends to incorporate trace elements useful as geochemical tracers, such as the REE, Y, and Hf. A number of characteristics of zircon encourage the preservation of internal isotopic and chemical variations, often on extremely fine scale, which provide valuable insight into thermal histories and past geochemical environments. The relative insolubility of zircon in crustal melts and fluids, as well as its general resistance to chemical and physical breakdown, often result in the existence of several generations of geochemical information in a single zircon grain. The fact that this information is so frequently retained (as evidenced through backscattered electron or cathodo-luminescence imaging that often reveal fine-scale zoning down to the sub-micron scale) has long suggested that diffusion of most elements is quite sluggish in zircon.

In this chapter, we present an overview of the findings to date from laboratory measurements of diffusion of cations and oxygen in zircon. Because of its importance as a geochronometer, attempts have been made to measure diffusion (especially of Pb) for over 30 years. But only in the last decade or so have profiling techniques with adequate depth resolution been employed in these studies, resulting in a plethora of new diffusion data. These findings have important implications for isotopic dating, interpretation of stable-isotope ratios, closure temperatures, and formation and preservation of primary chemical composition and zoning in zircon.

HISTORY—A BRIEF REVIEW OF BULK-RELEASE AND EARLY LOWER-RESOLUTION DIFFUSION MEASUREMENTS

Efforts have been made for some time to quantify and characterize diffusion in zircon, most notably of Pb, in deference to its significance in interpreting Pb isotopic signatures and refining understanding of thermal histories. As is evident from the summary of data plotted in Figure 1, there has historically been relatively little agreement between determinations of Pb diffusion rates, and values span a remarkably broad range (more than 10 orders of magnitude) in measured D. Many of these Pb diffusion studies have been considered in detail by Lee (1993); only brief discussion and summary are offered here.

The experiments of Shestakov (1969, 1972) and Magomedov (1970) relied upon bulk release methods, with the zircon crystals heated and the amount of Pb released recorded as a function of time. Such measurements are plagued by several difficulties, among them the presence of cracks, cleavage surfaces, dislocations and other features that might provide shortcut pathways for Pb transport through mineral grains. In addition, real mineral surfaces depart from model assumptions of ideal smooth surfaces, which would increase available surface area for exchange and affect calculated diffusivities. In these studies, Pb release did not obey a typical volume diffusion relationship, indicating the possibility of grain-boundary diffusion, and suggesting that surface volatilization as well as Pb migration might be a factor influencing Pb release patterns.

Sommerauer (1976) heated both crystalline and metamict zircons with PbO powder, and obtained an upper-limit estimate of Pb diffusion in the crystalline zircon based on an electron microprobe profile (or lack thereof, as Pb penetration was found to be <1 μm for an anneal of 2 days at

1529-6466/03/0053-0005$05.00

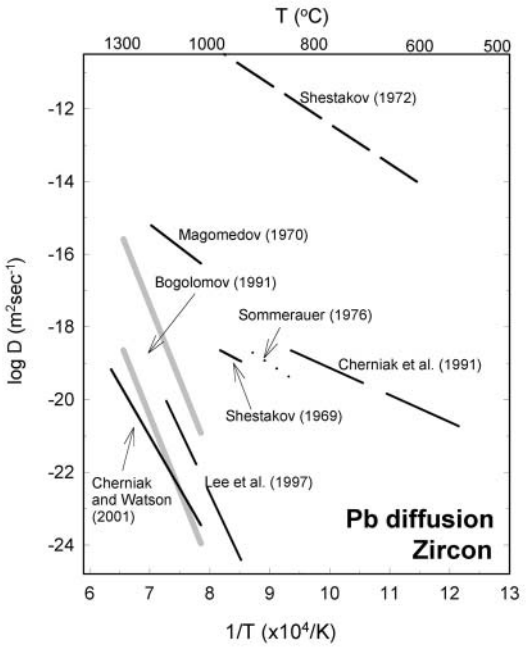

Figure 1. Summary of measurements of Pb diffusion in zircon. Sources for data are noted on the graph. Measurements gathered over more than three decades show relatively little agreement, and values span a remarkably broad range (more than 10 orders of magnitude) of diffusivities.

840°C). It is not surprising that an appreciable profile was not detected, since penetration distances would be <1 Å for these time-temperature conditions given values for diffusion parameters measured in recent work (Cherniak and Watson 2001).

The thermal evaporation experiments of Bogolomov (1991), which yield quite high activation energies (790-1180 kJ mol^{-1}) likely involved decomposition of zircon to ZrO_2 + SiO_2 during heating, as suggested by the work of Chapman and Roddick (1994). Pb loss in this case is not governed by simple volume diffusion but is instead controlled by the decomposition process and movement of the reaction front which would greatly enhance the mobility of Pb.

Measurements have also been made of the diffusion of noble gases, some of which are intermediate products in U-Pb decay sequences. Rn diffusion has been investigated in powdered zircon aliquots by measuring alpha activity of released ^{222}Rn (Gasparini et al. 1984). In that study, an activation energy for diffusion of 3.8 kJ mol^{-1} and pre-exponential factor of 6.4×10^{-18} m^2sec^{-1} were obtained over the temperature range 50 - 400°C. This extremely small activation energy may indicate that Rn diffusion was facilitated by alpha recoil damage to the zircon structure; the influence of radiation damage on diffusion is considered in more detail in subsequent sections.

Reiners et al. (2002) investigated He diffusion in zircon through a series of step-heating experiments. They obtained activation energies ranging from 145 to 185 kJ mol^{-1} (35 to 44 kcal mol^{-1}). However, they argue that temperature-dependent He release from the zircon crystals investigated is not consistent with thermally activated diffusion from a single diffusion domain, and that release patterns may reflect radiation damage to the zircon structure or the presence of distinct intracrystalline domains.

The studies outlined in this section point out some of the difficulties inherent in determining diffusivities from bulk release experiments, namely that factors other than volume diffusion contribute to and complicate interpretation of observed data. Measuring diffusion profiles directly removes some of this ambiguity, as it can be determined whether the profiles conform to appropriate solutions to the diffusion equation given the boundary conditions imposed by the experiment, or whether other non-diffusional processes are also taking place. One problem with diffusion measurements in zircon is that diffusion of most atomic species is extremely sluggish, so techniques of modest spatial resolution (e.g., EMPA) are of limited use, as was shown in Sommerauer's (1976) study. However, the development of SIMS, and the application of ion-beam techniques such as Rutherford Backscattering Spectrometry (RBS) and Nuclear Reaction Analysis (NRA) to geological studies, has permitted depth-profiling with depth resolution up to three orders of magnitude better than EMPA and thus made measurements of diffusivities of numerous elements in zircon possible.

CATIONS

In this section, we consider the diffusion of cations in zircon. Most of the experimental work on cation diffusion has involved the measurement of chemical diffusion. In chemical diffusion there

is a chemical potential gradient, and there will be a change in the total concentration of the diffusing element in the material and substitution of the diffusing species for another element in the mineral structure. In contrast, the oxygen diffusion experiments described in the next section represent self-diffusion, with simple exchange of oxygen atoms for other oxygen atoms in the material (with ^{18}O used as a tracer isotope to indicate the extent of exchange) producing no change in total oxygen concentration, only a change in the oxygen isotopic composition.

Pb

As noted previously, efforts to measure Pb diffusion in zircon extend back well over three decades. There are relatively few studies, and those only in the past decade or so, of Pb diffusion in zircon in which analytical techniques with superior depth resolution have been employed. The first of these was by Cherniak et al. (1991), in which RBS was used to characterize Pb profiles. This analytical method, although somewhat limited in sensitivity (to ~100 ppm for heavy elements) and isotope selectivity (except for lighter elements), is in many ways an excellent technique for measuring the diffusion of heavy elements in minerals such as zircon. Its superior depth resolution (to ~10 nm near-surface) permits the measurement of short diffusion profiles and quantification of the sluggish kinetics characteristic of cations in zircon.

In the Cherniak et al. (1991) study, Pb ions were implanted in natural zircon (from the Mud Tank carbonatite), and implanted samples were annealed under a range of time-temperature conditions, with resultant profiles measured by Rutherford Backscattering Spectroscopy. The process of ion implantation, however, produced significant amounts of damage to the zircon crystal, leading to apparently elevated diffusion rates for Pb, and a comparatively low activation energy for diffusion (142 kJ mol^{-1}). Interestingly, implantation of Pb at energies in the range of those used by Cherniak et al. (1991) creates damage comparable to that produced by alpha-recoil events in the decay of U to Pb in natural zircon (e.g., Ewing et al., this volume; Headley et al. 1982, Petit et al. 1987), so these results, as the authors then noted, provide a determination of Pb diffusion in zircons that have experienced significant radiation damage.

Lee et al. (1997) measured out-diffusion of Pb (as well as U and Th, to be discussed below) in a natural zircon from Sri Lanka. Experiments were run by immersing polished fragments of the zircon in a reservoir of molten NaCl to act as a "sink" for Pb, with ground zircon added to the salt in attempts to discourage zircon dissolution. Depth profiles were measured with SIMS, a technique that has been employed in diffusion studies in the geological sciences for a few decades (e.g., Giletti et al. 1978). They obtained an activation energy of 675 kJ mol^{-1} and pre-exponential factor of 3.9×10^{5} m^2sec^{-1} over the temperature range 900-1100°C.

More recently, Cherniak and Watson (2001) reported a thorough study of Pb diffusion in zircon, with diffusion experiments encompassing a broad range of experimental conditions and zircon compositions. The majority of the experiments were run on synthetic zircons (grown in a Li_2CO_3:MoO_3 flux) with a diffusant source consisting of a mixture of $PbSO_4$ and finely ground zircon. The zircon and this source were sealed under vacuum in silica glass capsules. Prepared capsules were then annealed in vertical 1-atmosphere tube furnaces at temperatures ranging from 1000 to 1300°C and times ranging from a few hours to several months. Profiles were measured with RBS. These are "in-diffusion" experiments, because a sample with a low initial concentration of the diffusing species (in this case, Pb) is annealed with a source enriched in the diffusant, resulting in a net increase in concentration of the diffusing species in the material. Example profiles are shown in Figure 2. A fit to the data from these diffusion experiments yielded the following Arrhenius relation:

$$D_{Pb} = 1.1\times10^{-1}\, exp(-550 \pm 30 \text{ kJ mol}^{-1}/RT) \text{ m}^2\text{sec}^{-1}$$

Experiments run with natural zircons crystals from the Mud Tank, Australia, carbonatite yielded diffusivities similar to those for the synthetic zircon crystals, suggesting that differences in trace-

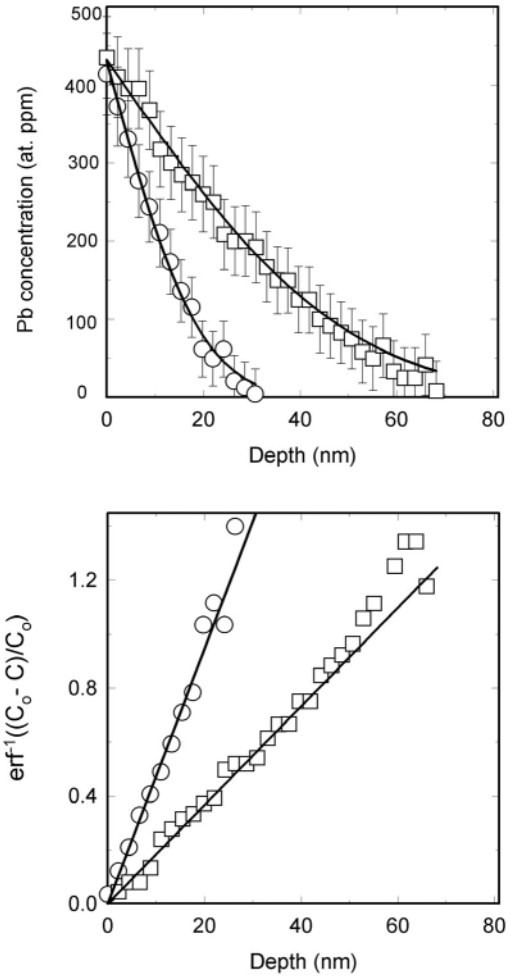

Figure 2. Typical diffusion profiles for Pb in-diffusion experiments measured by RBS. (a) The diffusion data are plotted with complementary error function curves. (b) The data are inverted through the error function. Slopes of lines are equal to $(4Dt)^{-1/2}$, where D is the diffusion coefficient and t is the duration of the experiment.

element compositions or defect concentrations have little influence on Pb diffusion in zircon. Similar diffusivities were obtained for zircon crystals oriented parallel and perpendicular to the *c*-axis, indicating little anisotropy in Pb diffusion (Fig. 3). In addition, measured diffusivities at a constant temperature (1200°C) agreed within experimental uncertainty for diffusion anneal times ranging over nearly an order of magnitude, providing evidence that what is being measured is volume diffusion of Pb (Fig. 3).

To investigate the effects of pressure on Pb diffusion, Cherniak and Watson (2001) ran experiments at 1.0 GPa in a piston-cylinder apparatus using pressure-sealing Pt liners inserted into holes in oxidized Ni cylinders (see Watson and Lupulescu 1993). The Pb sulfate/zircon source employed in the one-atmosphere experiments was also used in these high-pressure experiments. For "wet" high-pressure experiments, designed to investigate the effect of hydrous species on Pb diffusion in zircon, the $PbSO_4$/zircon source was mixed with finely ground zirconia and hydroxyapatite. Experiments were run at temperatures from 1100 to 1200°C, with both the "wet" and "dry" high-pressure experiments showing Pb diffusion rates similar to those for the one-atmosphere experiments (Fig. 3).

To further enhance the robustness of the data set, Cherniak and Watson (2001) performed a few types of "out-diffusion" experiments in addition to the "in-diffusion" experiments described above. "Out diffusion" experiments begin with a comparatively high concentration of the diffusing species in the sample material. Samples are annealed in a medium with lower concentration of the diffusant, which acts as a "sink;" net concentration of diffusant in the sample decreases as some of the diffusing species migrates out of the sample into the sink. For one of these experiments, a synthetic zircon was annealed with the $PbSO_4$ source in a silica glass capsule for 60 h at 1300°C, as in the "in-diffusion" experiments. The sample was removed from the source, cleaned, and the Pb uptake profile measured with RBS. It was then annealed in a Pt capsule surrounded by ground synthetic (Pb-free) zircon, which served as a sink for the Pb. The Pb distribution was again profiled with RBS, and a diffusion coefficient extracted from the Pb profile "relaxed" from its initial form by the second anneal. This experiment produced a diffusion coefficient that agreed within uncertainty with that of the in-diffusion experiments run at 1250°C (Fig. 3).

A second type of out-diffusion experiment was done with a natural zircon from Sri Lanka with relatively high Pb content (similar to the zircon sample used by Lee et al. 1997). Fragments of

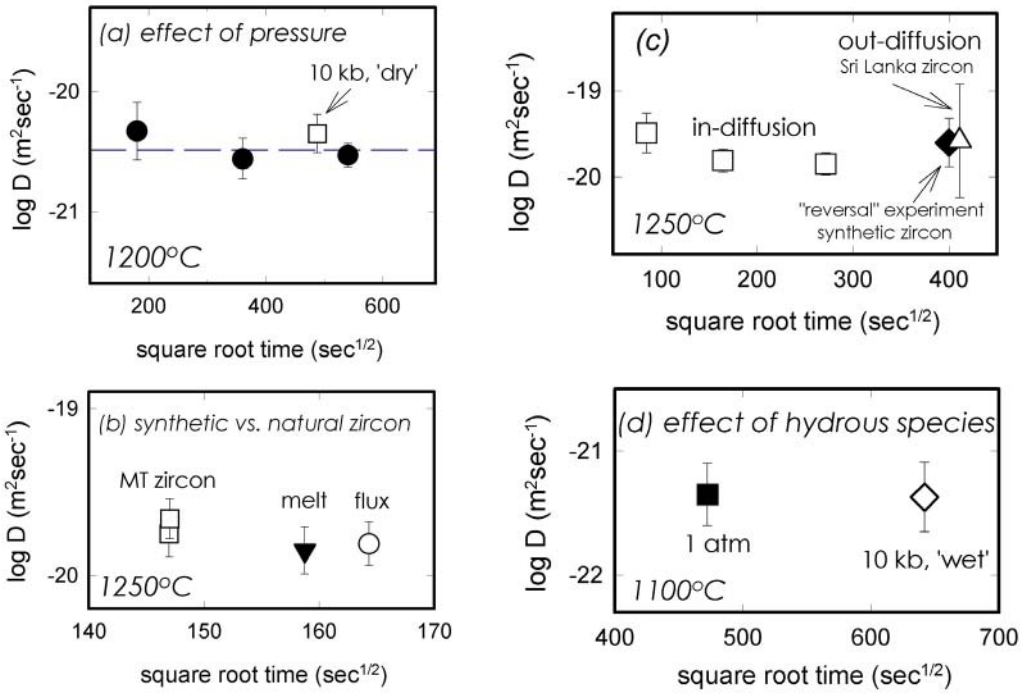

Figure 3. Time series for Pb diffusion anneals, and consideration of the influences of various factors on Pb diffusion in zircon from the study of Cherniak and Watson (2001). (a) Time series at 1200°C. diffusivities at constant temperature are generally quite similar for anneal times differing by a factor of 9. In addition, diffusion coefficients for experiments run at one atmosphere agree within uncertainty with that for an experiment run at 10 kbar, suggesting little influence of pressure on Pb diffusion in zircon. (b) Comparison of Pb diffusion for synthetic zircons grown in lithium carbonate/molybdenum oxide flux and in Pb silicate melt, and a natural zircon from the Mud Tank Carbonatite (MT). Zircons, regardless of origin or means of synthesis, have similar Pb diffusion rates. Further, measurements on the MT zircon indicate little anisotropy of Pb diffusion. (c) In-diffusion vs. out-diffusion. Diffusion coefficients for in-diffusion in synthetic zircon are comparable to that for Pb out-diffusion from a natural (Sri Lanka) zircon, and a "reversal" experiment (described in text) on a synthetic zircon. (d) Wet vs. dry diffusion. Diffusion rates at 1100°C for experiments at 1 atmosphere and at 10 kbar in the presence of water agree within experimental uncertainty, and indicate that the presence of hydrous species has little influence on Pb diffusion in zircon.

the zircon were polished to 0.05 μm using gamma alumina, and annealed overnight at 900°C in air in an open Pt capsule order to repair surface damage that might be a consequence of the polishing process. The specimens were then annealed at higher temperatures (one at 1250°C, another at 1470°C) in Pt capsules surrounded by finely powdered synthetic zircon as a sink for Pb. A third type of out-diffusion experiment was run using Pb (and P) doped zircons grown in a PbO-SiO_2-ZrO_2-P_2O_5 melt (Watson et al. 1997). The zircon grains were annealed in Pt capsules at 1500°C, again surrounded by finely ground synthetic (undoped) zircon. For the latter two types of out-diffusion experiments, Pb profiles of the highest-temperature experiments (i.e., 1470 and 1500°C) were measured with an electron microprobe; that for the lower temperature experiment was measured with RBS. The latter out-diffusion experiment on the natural zircon from Sri Lanka yielded a diffusivity entirely consistent with the other measurements of Pb diffusion made at the same temperature in this study (Fig. 3), and, even with the large uncertainty taken into account (due to the relatively small number of counts in the RBS spectra produced by Pb and the limited depth range over which the Pb signal could be followed due to the presence of Hf), was still found to be significantly smaller than the diffusivities measured by Lee et al. (1997), in which a similar experimental protocol (i.e., out-

diffusion of Pb from a natural zircon into a Pb-poor medium) was employed.

The 1470°C experiment on the Sri Lanka zircon, and the out-diffusion experiment on the Pb doped synthetic zircon (at 1500°C), were also consistent with the lower-temperature results from this study, as they lie on an up-temperature extrapolation of the Arrhenius line determined from the out-diffusion data gathered at temperatures 1000-1300°C (Fig. 4). A "global" fit to all the Cherniak and Watson (2001) data yields an activation energy of 545 ± 25 kJ mol^{-1} and pre-exponential factor of 7.8×10^{-2} m^2sec^{-1} (log D_o = -1.11 ± 0.88), for temperatures spanning 500°C and diffusivities ranging over 6 orders of magnitude (Fig. 3).

The differences in Pb diffusion parameters (Fig. 1) determined in the most recent depth profiling studies (Lee et al. 1997, Cherniak and Watson 2001) warrant a brief discussion. The Lee et al. (1997) Arrhenius equation for a Sri Lanka zircon is based on only a few data points (7 points, at only three temperatures) acquired in experiments involving a Pb sink (molten NaCl) known to be reactive with zircon. Their study included a modest time series (i.e., experiments of differing duration at a single temperature), one of the standard tests to confirm diffusion-controlled transport. However, the experiment durations in their time series vary by a factor of only 1.8, leading to a small difference in expected diffusive transport distance (~1.3, as diffusion distance *x* scales with the square root of time), which is not definitive. Judging from the diffusivities and durations reported for experiments at 900°C, the SIMS depth profiles at this temperature were only a few nanometers long, which challenges the spatial resolution of the SIMS method and would lead to uncertainties in diffusivities inconsistent with the values reported. The Cherniak and Watson (2001) study, in contrast, included a rigorous time series (9-fold variation in experimental duration, Fig. 2), experiments involving both in- and out-diffusion of Pb, three different zircons (both synthetic and natural, including one out-diffusion experiment on a Sri Lanka zircon), and two different analytical methods (RBS and EPMA).

Substitutional processes involving Pb

An important consideration in Pb diffusion is the role of coupled substitution in Pb exchange, and whether the type of exchange process involved affects diffusivities. Such dependence of D on the substitutional process has been noted for REE diffusion in apatite, for example, where diffusion with coupled substitutions involving highly charged cations (e.g., REE^{+3} +Si^{+4} → Ca^{+2} + P^{+5}) proceeds much more slowly than simple REE^{+3}→ REE^{+3} exchange (Cherniak 2000). Since Pb cations will most commonly be found in nature in the +2 valence state (e.g., Otto 1966,

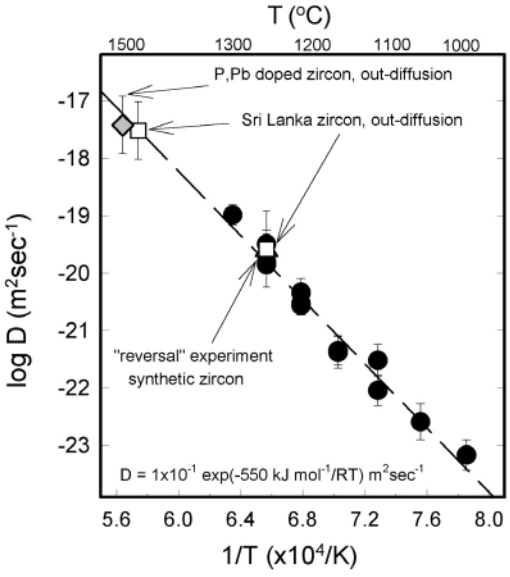

Figure 4. Arrhenius plot of Pb diffusion in zircon, from the study of Cherniak and Watson (2001). Plotted are in-diffusion experiments on synthetic and natural (Mud Tank) zircon, and out-diffusion and "reversal" experiments. The line is a least-squares fit to the data from 1000-1300°C; Arrhenius parameters extracted from the fit are: activation energy 550 kJ mol^{-1}, and pre-exponential factor 1.1×10^{-1} m^2sec^{-1}. Also plotted are diffusivities from high-temperature out-diffusion experiments on natural (Sri Lanka) zircon and zircon grown from Pb silicate melt doped with phosphorus. These data lie on an up-temperature extrapolation from the lower-temperature measurements, illustrating the consistency between these data sets.

Watson et al. 1997), other cations (or defects such as oxygen vacancies) must provide charge balance. This is also a matter of concern when applying results from the laboratory to Pb diffusion in nature, since most Pb in natural zircon is a result of radioactive decay. Although radiogenic Pb may initially occupy locations other than "normal" structure sites due to displacement as consequence of the multistage decay process, as soon as Pb atoms become mobile (and over a very short length scale) they will occupy sites in a manner comparable to common Pb, and therefore should diffuse in a similar way. However, there is the possibility that Pb diffusion rates may differ if there are other species involved in a coupled exchange, and if the other species are rate-limiting in the diffusion process.

Because there is relatively little latitude in zircon for a broad range of substituent cation species on either the *Zr* or *Si* sites, we consider the possibility of either S^{+6} or P^{+5} on the *Si* site to charge-balance Pb on the *Zr* site (e.g., $Pb^{+2} + 2P^{+5} \rightarrow Zr^{+4} + 2Si^{+4}$; $Pb^{+2} + S^{+6} \rightarrow Zr^{+4} + Si^{+4}$). The study of Watson et al. (1997) has shown that significant amounts of Pb can be incorporated into zircon crystals grown from a melt when P is present. Zircon crystals grown from PbO-SiO_2-ZrO_2 melts incorporate little Pb (<1 ppm; Watson et al. 1997). However, when phosphorus (~several wt % P_2O_5) is included in the melt, Pb concentrations in the resulting zircons are orders of magnitude higher (~1000 ppm; Watson et al. 1997). This finding is also consistent with the observation in natural zircon crystals that high levels of common Pb are often associated with the presence of P (e.g., Watson et al. 1997).

The other candidate is sulfur in the hexavalent state. While sulfur has been reported in chemical analyses of zircon (e.g., Speer 1982), it may be due to inclusions of other minerals such as galena. It is less clear that it is ubiquitous in zircon itself, or whether it might be present in sufficient quantity to play some charge-compensating role. Conceivably, Pb could be charge compensated in substituting for Zr through a substitution of S (in the hexavalent state) for Si. In the interest of thoroughness, Cherniak and Watson (2001) explored this possibility by measuring S on a number of their zircon samples from experiments using the $PbSO_4$ diffusant source, with NRA using the 6.90 MeV resonance of the $^{32}S(\alpha,p)^{35}Cl$ reaction (Soltani-Farshi et al. 1996). These analyses showed no evidence of sulfur above detection limits of about 50 ppm (atomic), indicating that sulfur played no significant role in the exchange process for Pb diffusion, even where abundant S was available in the environment.

In the experiments of Cherniak and Watson (2001), Pb diffusivities at a given temperature were found to be quite similar for the different types of experiments in which diffusion via different mechanisms might be possible (i.e., Pb in-diffusion using a $PbSO_4$ source, out diffusion from synthetic P- and Pb-doped zircon, out-diffusion from natural Pb-bearing Sri Lanka zircon). This suggests that several factors that might have been heretofore suspected of affecting Pb diffusion in zircon seem to exert little significant influence. If either P^{+5} or S^{+6} played a compensating role, it would be most likely the case that Pb diffusion would be rate limited by the diffusion of these highly charged cations, so Pb diffusivities would differ depending on the substitutional process involved. Given the apparent similarities of Pb diffusion rates over this range of conditions, it seems likely that divalent Pb is charge compensated in another way, possibly by oxygen vacancies (O^{-2} centers), as may be the case for the REEs in zircon (Cherniak et al. 1997a, and discussion in the next section). Diffusion of oxygen, even under dry conditions (Watson and Cherniak 1997), is also faster than diffusion of Pb in zircon (see Fig. 10 below), so movement of Pb would then be expected to be the rate-limiting factor in Pb diffusion.

Diffusion systematics of trivalent cations

Diffusion measurements on the trivalent cations have concentrated on the rare earth elements because of their importance as indicators of geochemical processes. Cherniak et al. (1997a) measured diffusion rates of Sm, Dy and Yb in synthetic zircon, and natural zircon from the Mud Tank carbonatite. Experiments were run at 1-atm with rare-earth phosphate powder sources, over temperatures ranging from 1150 to 1650°C; profiles were analyzed with RBS and electron microprobe.

Little evidence of anisotropy was noted for experiments run on zircons cut parallel and perpendicular to *c*-axis (as was also observed in the case of Pb), and Dy diffusivities in natural and synthetic zircons were quite similar. Over the temperature range 1150-1400°C (1150-1650°C for Yb) the following Arrhenius relations were obtained:

$D_{Sm} = 2.9\times10^{8} exp(-841 \pm 57\ kJmol^{-1}/RT)\ m^2sec^{-1}$
$D_{Dy} = 2.3\times10^{5} exp(-734 \pm 35\ kJmol^{-1}/RT)\ m^2sec^{-1}$
$D_{Yb} = 3.8\times10^{4} exp(-691 \pm 47\ kJmol^{-1}/RT)\ m^2sec^{-1}$

It is evident from these expressions that diffusion rates vary among the rare earth elements (REEs) in a systematic manner: Diffusion rates of the heavy rare earths (with smaller ionic radii) are faster than the larger lighter REE (Fig. 5). In addition, activation energies for diffusion increase when going from the smaller heavy REE to the light REE. To attempt to quantify this observed behavior, we plot ionic rare-earth ionic radius (8-fold coordination; Shannon 1976) against the activation energy (Fig. 6a) and the log of the pre-exponential factor D_o (Fig. 6b). Both activation energy and log of the pre-exponential factor fall along second-order polynomial curves, so the data permit us to predict diffusivities for the other REEs at a given temperature as a function of ionic radius. Curves generated with the derived expression for various temperatures are plotted in Figure 7. At 1200°C, there is a difference of about 2 orders of magnitude in diffusivities of Lu and La. At lower temperatures, because of predicted differences in activation energies, the disparity between diffusivities of the light and heavy REEs becomes more pronounced.

Since there are only three points to constrain the lines, it cannot be assured that the REEs as a group define the simple relationship discussed above and there may not necessarily be any physical significance attached to it. It might be argued that activation energies are a function not only of site energy but also porosity of the structure (e.g., Dowty 1980) and that the larger REEs would therefore have greater difficulty in moving through the relatively compact and stiff zircon structure.

Van Orman et al. (2001) developed a simple elastic model for diffusion to qualitatively describe observed dependencies of diffusion of like-charged cations (such as the REE) on ionic radii. This model, adapted from the work of Mullen (1966) and Zener (1952) assumes that the motion energy of diffusing ions is due to elastic strain, and considers the difference in motion energy that results from the difference between the size of an impurity ion and the ideal site radius. This quantity, expressed as a size factor δ, where $\delta = (r_{imp} - r_{site})/r_o$ with r_{imp} the impurity ion radius, r_{site} the ideal site radius, and r_o the average cation-anion distance. Activation

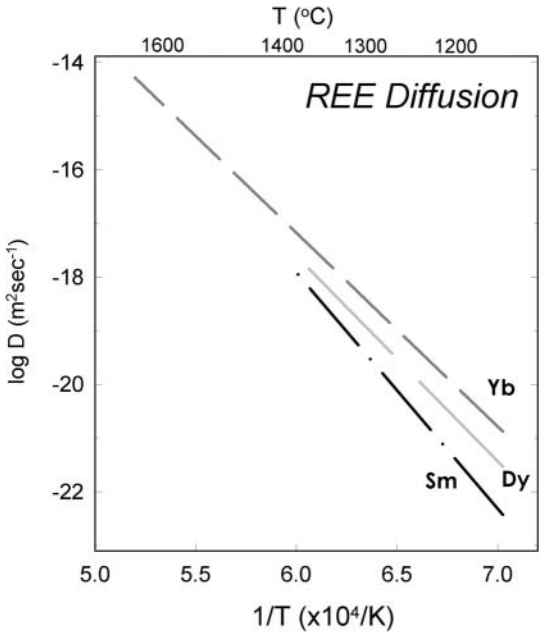

Figure 5. Summary of REE diffusion data for zircon, from the study by Cherniak et al. (1997a). REE diffusivities display a consistent trend of increasing diffusivity and decreasing activation energy for diffusion when going from the light to heavy rare earths (and larger to smaller ionic radii). Arrhenius parameters for the REE are: Sm - $E_a = 841\pm57$ kJ mol^{-1}, $D_o = 2.9\times10^{8}$ m^{2}sec^{-1}; Dy - $E_a = 734\pm35$ kJ mol^{-1}, $D_o = 2.3\times10^{5}$ m^{2}sec^{-1}; Yb - $E_a = 691\pm47$ kJ mol^{-1}, $D_o = 3.8\times10^{4}$ m^{2}sec^{-1}.

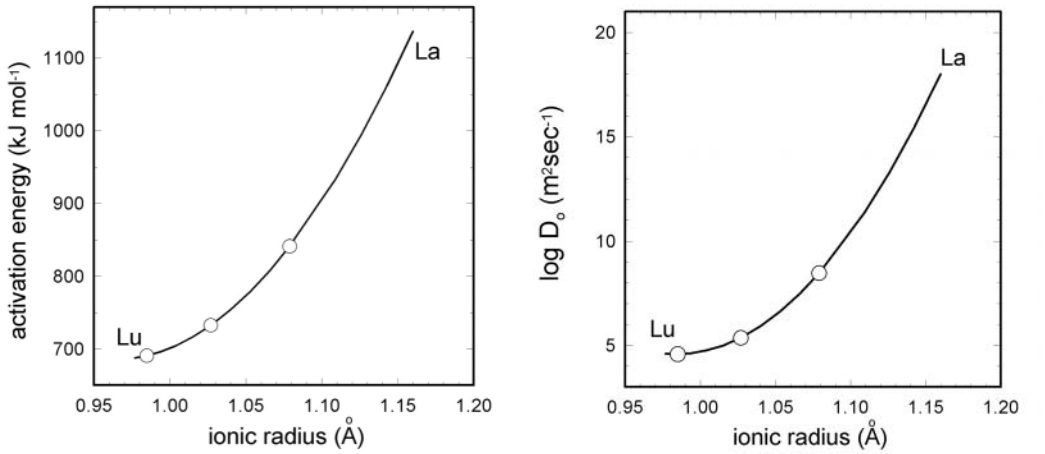

Figure 6. Correlation of activation energy and pre-exponential factor with ionic radius for the rare earth elements, from the study of Cherniak et al. (1997a). Lines in (a) and (b) are second-order polynomial curves passing through the data (symbols) extended over the full range of the rare earths. (a) Activation energy. The relationship between ionic radius (r, in Å) and activation energy (E_a, in kJ mol^{-1}) expressed by the curve is: $E_a = 1.15\times10^4 - 2.25\times10^4 r + 1.17\times10^4 r^2$. (b) Pre-exponential factor. The relationship between ionic radius (r, in Å) and log of the pre-exponential factor (D_o, in m^2sec^{-1}) expressed by the curve is: $\log D_o = 4.28\times10^2 - 8.60\times10^2 r + 4.37\times10^2 r^2$.

energies for diffusion may be larger for cations larger than the ideal size. A relationship relating the activation energy to ion size can be derived if one assumes that a large proportion of the energy expended in an atomic jump is due to lattice strain, so cation size can then be related to the motion energy of a cation (i.e., E_m) as follows:

$$E_m = E_m^o\{1 + 2[\delta(1 - 1/\sqrt{2})^{-1} - \delta^2(1 - 1/\sqrt{2})^{-2}]\} \quad (1)$$

Here, E_m^o refers to the motion energy for an ion with an ideal radius. This equation describes a parabola, with a minimum value when $\delta = 0.146$. In the expression above, the minimum motion energy for zircon will occur for an ionic radius of 0.116 nm, which corresponds to the ionic radius of La^{+3} in 8-fold coordination (Shannon 1976). However, it is counterintuitive to assume that motion energies will increase with increasing ionic radius beyond this minimum; the data presented here explore only the region where $\delta < \delta_{min}$ so we can offer no comment on the diffusional behavior of cations beyond this size limit (and La is of course the largest of the REE).

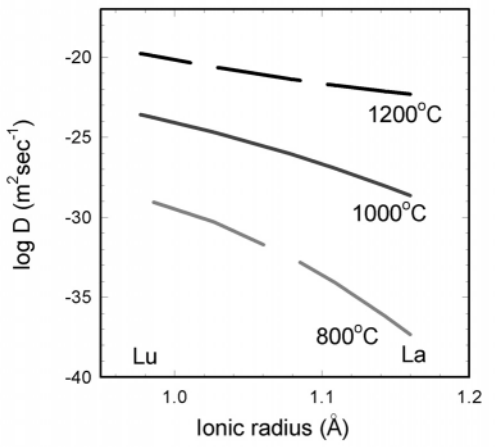

Figure 7. Plot of REE diffusivities at various temperatures as a function of ionic radius. Diffusivities are calculated using the expressions discussed in the text and presented in Figure 6. Because of the differences in predicted activation energies, differences between diffusivities of the light and heavy rare earths grow increasingly larger with decreasing temperature.

If we assume diffusion via an intrinsic vacancy mechanism, the activation energy for diffusion will consist of energies for vacancy formation and migration. Energies for vacancy formation will be independent of ionic radii, so the dependence on ionic radii will be present in the migration

energy. If we use the theoretical Zr vacancy formation energy (~600 kJ mol^{-1}; Williford et al. 1999) and take E_m^o in the above expression as equal to the Zr vacancy migration energy (~110-130 kJ mol^{-1}; Williford et al. 1999), ignoring for the moment any charge dependence of migration energy. If we use the latter value in Equation (1) above to estimate migration energies for the rare earths, and sum with the vacancy formation energy to estimate activation energy, we obtain values ranging from 790 kJ mol^{-1} (for Sm) to 695 kJ mol^{-1} (for Yb), compared with the experimental results of 841 to 691 kJ mol^{-1}, indicating reasonable agreement of experimental and theoretical findings.

Because the pre-exponential factor depends on the temperature derivative of the material's bulk modulus (e.g., Zener 1952, Van Orman et al. 2001) as well as the ionic radius, it is expected that variations in diffusivities with ionic radius in zircon will be greater than for less rigid mineral structures. This appears to be the case under some circumstances, as REE diffusion in clinopyroxene (Van Orman et al. 2001) displays a much less pronounced dependence on ionic radii than zircon. In other minerals, including plagioclase (Cherniak 2002), apatite (Cherniak 2000), fluorite (Cherniak et al. 2001) and calcite (Cherniak 1998b) there is little evidence of dependence of REE diffusivities on ionic radii. However, some minerals with comparatively stiff structures, such as aluminosilicate (Van Orman et al. 2002) and aluminate garnets (Cherniak 1998a), show little variation of REE diffusivities with ionic radii, indicating that the simple elastic model cannot provide broad quantitative predictions of diffusivities for a range of minerals. And although this model can describe qualitative trends for diffusion of the REE in zircon (and clinopyroxene) it predicts larger variances among REE diffusivities than the experimental data indicate.

Substitutional processes for trivalent cations

The xenotime-type substitution (i.e., $REE^{+3} + P^{+5} \rightarrow Zr^{+4} + Si^{+4}$) is commonly reported in natural zircon crystals (e.g., Speer 1982, Hinton and Upton 1991), and may be a means for charge compensation during REE diffusion. The substitutional processes involved in REE exchange were investigated by Cherniak et al. (1997a) through complementary NRA and RBS measurements of phosphorus and the rare earths, respectively, with phosphorus measured using the 3.048 and 3.640 MeV resonances of the $^{31}P(\alpha,p)^{34}S$ nuclear reaction (McIntyre et al. 1988). Measurements of P on several of the zircon samples show that there is no phosphorus above detection limits (~600 atomic ppm).

The finding that phosphorus has at most a minor involvement in REE diffusion is consistent with the observed trend of increasing REE diffusivity with decreasing ionic radius. If coupled REE + P diffusion were occurring, diffusion would likely be rate-limited by pentavalent P rather than the trivalent REEs, so major differences in REE diffusivities would be unlikely. Oxygen, on the other hand, diffuses much more rapidly than the REEs (e.g., at 900°C, oxygen diffuses about 3 orders of magnitude faster than Yb; Watson and Cherniak 1997), so, as in the case of Pb diffusion, oxygen defects are a potential candidate for charge compensation of the REE in zircon. The formation of oxygen vacancies (O^{-2} centers) is possible at high concentrations of REE when there is a high probability of two REEs in adjacent *Zr* sites. In addition, the calculated energy for oxygen vacancy migration (0.99-1.16 eV; Williford et al. 1999) is considerably less than that for oxygen vacancy formation (5.6 eV, Crocombette 1999), so while significant numbers of static *oxygen* site vacancies are unlikely to persist in the zircon structure (e.g., Hanchar et al. 2001), they may be present (and mobile) in sufficient quantity to facilitate exchange not charge-balanced by P. Because of the difficulty in measuring relatively small changes in oxygen concentration, however, it is not possible to directly determine whether the REEs are predominantly compensated by oxygen defects.

Other possibilities do exist. Zircons that contain up to 0.8 mol % rare earth elements have been synthesized in the absence of phosphorus (Hanchar et al. 2001), a concentration on order of the maximum REE uptake measured in the Cherniak et al. (1997a) diffusion experiments (REE surface contents ranging from 1 to 0.05 mol %). In these cases, it has been determined that some charge compensation of the REE occurs via inclusion of Li^{+1} and Mo^{+6} (both species are present in the flux used to grow the zircons) interstitially. Watson (1980) also synthesized zircon crystals with high

REE contents in felsic peralkaline melts with no phosphorus present, a system more closely resembling that found in nature than the lithium metasilicate-molybdenum oxide flux used by Hanchar et al. (2001). In some natural zircon crystals, it has also been found that at least 50% (on an atomic basis) of REE-Zr substitutions are not compensated by phosphorus or pentavalent cations (Hinton and Upton 1991). Under hydrous conditions, REE can be compensated by substitution of hydroxyl groups $(OH)^-$ for $(SiO_4)^{4-}$ (e.g., Caruba et al. 1974, Medenbach 1976, Robinson 1979), with the formula $(Zr_{1-y}REE_y)(SiO_4)_{1-x}(OH)_{4x-y}$, or by protonation of the O^{2-} ions of the $(SiO_4)^{4-}$ groups (i.e, $SiO_{4-x}(OH)_x)_{x-4}$, or simply by the presence of interstitial H^+ (see Hanchar et al. 2001 for a discussion of possible substitution mechanisms). It remains unclear whether other species in natural zircons might provide charge balance.

Tetravalent cations

Diffusion of tetravalent cations (Hf, Th and U) was characterized by Cherniak et al. (1997b). Experiments were done by annealing synthetic zircon in Pt capsules with a source material. For Hf diffusion, the source consisted of a mixture of HfO_2 and SiO_2 powders in proportions of stoichiometric hafnon ($HfSiO_4$). The source for Th experiments was a mixture of ground synthetic thorite and zircon, while for U diffusion experiments it consisted of a mixture of UO_2, SiO_2, and ground synthetic zircon. Diffusion profiles were measured with RBS. Over the temperature range 1400-1650°C, the following Arrhenius relations were obtained (Fig. 8):

$D_{Th} = 9.6\times10^{1} exp(-792 \pm 34 \text{ kJ mol}^{-1}/RT) \text{ m}^2\text{sec}^{-1}$
$D_{U} = 1.6 exp(-726 \pm 83 \text{ kJ mol}^{-1}/RT) \text{ m}^2\text{sec}^{-1}$
$D_{Hf} = 8.6\times10^{2} exp(-812 \pm 54 \text{ kJ mol}^{-1}/RT) \text{ m}^2\text{sec}^{-1}$

The results for Hf diffusion are consistent with the "upper limit" value of 10^{-19} m^2sec^{-1} at 1600°C, determined by Suzuki et al. (1992) using electron microprobe analysis of synthesized zircon-hafnon couples annealed at high temperatures. Lee et al. (1997) measured apparent out-diffusion of U and Th from a natural zircon from Sri Lanka containing ~240 ppm U and 20 ppm Th, with Pb profiles measured as well (as discussed above). These experiments were run by immersing zircons in a reservoir of molten NaCl containing ground zircon in attempts to minimize dissolution, with diffusive-loss profiles measured by SIMS. They ob-

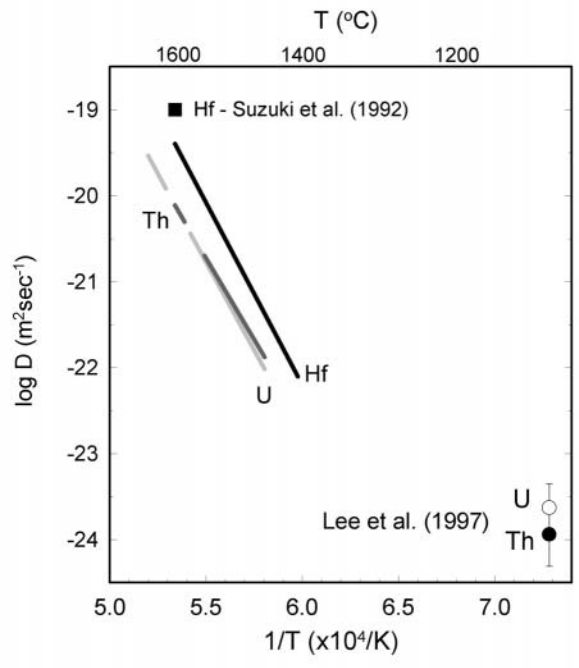

Figure 8. Arrhenius plot of U, Th and Hf diffusion in zircon from the study of Cherniak et al. (1997b). Measurements are for diffusion perpendicular to c. The lines are least-squares fits to the data. Arrhenius parameters for these fits: Hf - activation energy 812 kJ mol^{-1}, pre-exponential factor 1.6×10^3 m^2sec^{-1}. U - activation energy 726 kJ mol^{-1}, pre-exponential factor 1.6 m^2sec^{-1}. Th - activation energy 792 kJ mol^{-1}, pre-exponential factor 8.6×10^2 m^2sec^{-1}. Also plotted is the upper-limit estimate for Hf diffusion at 1600°C from the study of Suzuki et al. (1992), and the data reported by Lee et al. (1997) for U and Th diffusion at 1100°C.

tained diffusivities of 1.16×10^{-24} m^2sec^{-1} (log D = -23.94 ± 0.37) for Th, and 2.34×10^{-24} m^2sec^{-1} (log D = -23.63 ± 0.28) for U at 1100°C. However, given the diffusion times and calculated diffusivities reported in their study, the lengths of the resulting diffusion profiles would be on the order of only a few tens of angstroms, and so may not be easily quantified with the SIMS instrument used in their measurements.

Although Cherniak et al. (1997b) could not measure diffusivities at 1100°C, down-temperature extrapolation using their Arrhenius relations yield 6.8×10^{-29} m^2sec^{-1} for Th and 3.1×10^{-28} m^2sec^{-1} for U, or about 4 orders of magnitude slower than the Lee et al. (1997) results. A possible reason for this discrepancy may be that the molten salt medium used for a "sink" for the diffusant in the Lee et al. (1997) experiments caused incongruent dissolution and recrystallization of the zircon surface despite the presence of ground zircon in the melt. Thus, concentration gradients may have been produced by a reaction rather than simple volume diffusional exchange.

As in the case of the REE, Cherniak et al. (1997b) find a systematic variation of diffusion rates for the tetravalent cations with ionic radius, where diffusivities increase with decreasing ionic radius. Efforts to quantify this observed trend were first made by Cherniak et al. (1997b), where they "normalized" pre-exponential factor for the U, Th, and Hf diffusion data by assuming a constant activation energy (795 kJ mol^{-1} [190 kcal mol^{-1}]) for all three cations. This was considered a reasonable approach since, in contrast to the REE, no clear systematic dependence of activation energy for diffusion on ionic radii could be determined. However, it is likely that there is some dependence does exist, but the limited range in 1/T that could be sampled in these measurements does not allow for strong constraints. We instead take into consideration variations in both D_o and activation energy by plotting log of the diffusivities themselves (calculated at a temperature included in the range over which diffusivities were measured) against ionic radii of the tetravalent cations. These data can be fit (albeit somewhat arbitrarily) to a second-order polynomial (Fig. 9). The data may then be used to predict diffusivities for other tetravalent cations as a function of ionic radius. Other functional forms can be plotted against the data, but predicted pre-exponential factors in such cases differ little (up to [and in most cases much less than] 0.1 log unit) over a reasonable range of ionic radii. Further, the parabolic function form is consistent with a simple elastic model, which can be used to qualitatively describe diffusional behavior as a function of cationic radius.

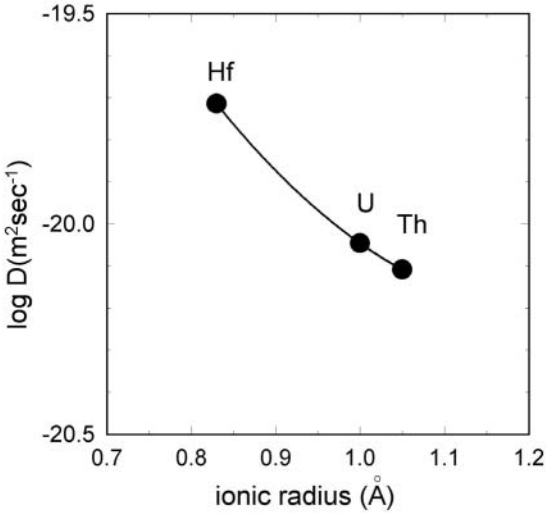

Figure 9. Correlation of diffusivities (at 1600°C) with ionic radius for the tetravalent cations U, Th and Hf in zircon. The data fall along a second-order polynomial curve representing the following relationship between ionic radius (r, in Å) and log of the diffusivity (D_o, in m^2sec^{-1}): $\log D = -15.47 - 7.74\, r + 3.16r^2$.

The differences in diffusivities among these tetravalent cations are less pronounced than among the trivalent REEs. A stronger dependence on ionic radius of both the pre-exponential factor and activation energy (Cherniak et al. 1997a) is evident in the latter case. The reason for this is not yet clear. It is possible that the larger deviation of the LREE from the size of the Zr ionic radius may contribute to this stronger dependence. Trivalent REEs from La to Gd all have ionic radii (8-fold coordination, +3 valence) larger than the largest tetravalent cation (Th) investigated.

While dependence of diffusivities on ionic radii among tetravalent cations is much less significant than for the REE, the tetravalent cations do exhibit slower overall diffusivities than the trivalent REE. The

REEs diffuse 3-5 orders of magnitude faster than the tetravalent cations. Such pronounced variations in diffusivities with cation charge have been noted in other mineral systems. For example, K diffusion in orthoclase (Foland 1974) is more than three orders of magnitude faster than Sr and Pb diffusion (Cherniak and Watson 1992, Cherniak 1995). In plagioclase, univalent cations (Na and K) diffuse 3-6 orders of magnitude faster (Giletti and Shanahan 1997) than divalent cations Sr (Cherniak 1996, Cherniak and Watson 1994, Giletti and Casserly 1994), Pb (Cherniak 1995), and Ba (Cherniak 2002a) for feldspars of a given compositional range, which in turn diffuse 1-4 orders of magnitude faster than the trivalent REE (Cherniak 2002b).

Cation diffusion in zircon—a general summary

A consideration of some trends. As outlined above, there now exists a body of data for diffusion of various cations and anions in zircon (Fig. 10). Certain systematic behaviors have been observed among trivalent and tetravalent cations. For cations of a given charge, diffusivities increase with decreasing ionic radius. The REE, for example, exhibit marked variation in diffusion rates from the light to heavy REE, with diffusion coefficients of Lu and La expected to differ by roughly two orders of magnitude. Among tetravalent cations, Hf diffuses more rapidly than U or Th, but these differences are not as pronounced as those found among trivalent cations. The influence of cation charge is also great; the (trivalent) REEs diffuse 3-5 orders of magnitude faster than tetravalent cations in zircon. Pb likely exists in the divalent state in these diffusion studies, and in zircons in nature as well, since Pb is stable in the +4 valence state at elevated temperatures only under conditions of very high f_{O2} (e.g., Otto 1966, Watson et al. 1997). At the same time, the ionic radius of Pb^{+2} is quite large (1.29 Å in 8-fold coordination; Shannon 1976). It appears in the case of Pb that these two factors, i.e., lower charge tending to increase diffusion rates and larger ionic radius tending to reduce them, provide competing influences.

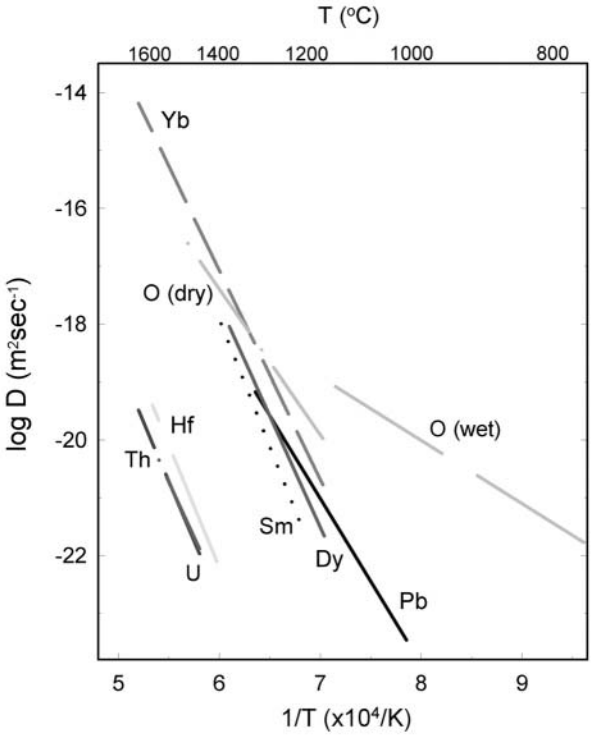

Figure 10. Summary of diffusion data for various cations and anions in zircon. Sources for data: Yb, Dy, Sm - Cherniak et al. (1997a); Hf, U, Th - Cherniak et al. (1997b); oxygen - Watson and Cherniak (1997); Pb - Cherniak and Watson (2001).

Possible mechanisms for diffusion. The results from these experimental studies of cation diffusion, as well as recent theoretical determinations of energies of formation and migration of various defects in zircon (Williford et al. 1999, Crocombette 1999, Meis and Gale 1998), permit us to speculate on possible mechanisms for diffusion. For a few reasons it appears most likely that cations diffuse via an intrinsic vacancy mechanism. Diffusivities for both synthetic and natural zircon crystals with varying concentrations of aliovalent impurities are quite similar, which suggests that extrinsic cation vacancies are an unlikely mechanism, because the concentrations of these defects

would be proportional to the concentration of the dominant aliovalent impurity (e.g., P^{+5}). Further, theoretically-determined Zr vacancy migration energies (Williford et al. 1999) range from 1.16-1.38 eV (110-130 kJ mol^{-1}), considerably smaller than the activation energies for cation diffusion. However, energies for creation of Zr vacancies by Schottky defect formation are 6.2 eV/defect (600 kJ mol^{-1}) and 12.28 eV/defect (1190 kJ mol^{-1}) for Frenkel defect formation (Williford et al. 1999, He and Cormack 1999), so the experimental activation energies are consistent with an intrinsic regime reflecting energies of both formation and migration of Zr vacancies. Zr intersitials can be reasonably ruled out as unfavorable because of their very high estimated energy of formation (18.0 eV [1740 kJ mol^{-1}]; Crocombette 1999). Calculations by Meis and Gale (1998) using empirical potentials for zircon and applying static transition state theory, estimate an activation energy for diffusion of U^{+4} (via a vacancy mechanism) in zircon of 5.9-9.4 eV (570-900 kJ mol^{-1}), consistent with experimentally determined activation energies for diffusion of tetravalent cations (e.g., 726-812 kJ mol^{-1}).

OXYGEN DIFFUSION

Experimental results

Oxygen diffusion in zircon was first measured by Muehlenbachs and Kushiro (1975), using a bulk-diffusion method with zircon heated in the presence of ^{18}O-enriched gas. At 1300°C, they obtained a diffusivity of ~10^{-19} m^2sec^{-1}.

More recently, oxygen diffusion has been measured under both dry and hydrothermal conditions, using ^{18}O enriched sources (Watson and Cherniak 1997) and direct characterization of ^{18}O diffusional uptake profiles with NRA using the $^{18}O(p,\alpha)^{15}N$ reaction. The dry diffusion experiments were run by sealing ^{18}O-enriched quartz powder with a polished zircon specimen in Pt capsules, with a small amount of Zr metal powder added to scavenge atmospheric N_2 and O_2 sealed in the Pt capsule upon welding, which might cause capsule rupture.

Hydrothermal experiments were run in both cold-seal pressure vessels and solid-media piston-cylinder apparatus, using a source consisting of both the ^{18}O enriched quartz and ^{18}O enriched water, to simulate near-surface and lower-crustal conditions, respectively. Cold-seal runs covered the pressure range ~7-83 MPa and temperature range 767-1003°C, with piston-cylinder runs at pressures from 0.4 to 1.0 GPa and temperatures ranging from 925 to 1160°C.

For the dry experiments, the following Arrhenius relation was obtained (Fig. 11):

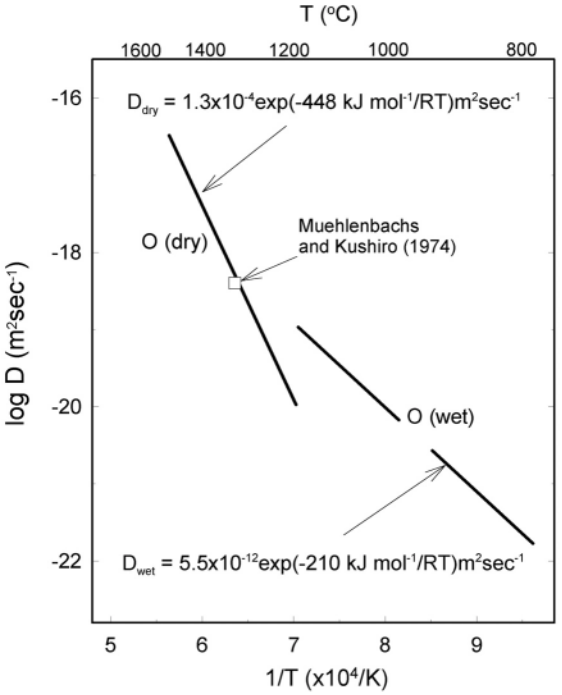

Figure 11. Comparison of dry and wet diffusion results from the work of Watson and Cherniak (1997). Also on the plot is the datum for oxygen diffusion under dry conditions measured by Muehlenbachs and Kushiro (1974). Diffusion of oxygen under dry conditions is slower and has a higher activation energy for diffusion than oxygen diffusion under wet conditions (448 vs. 210 kJ mol^{-1}), a finding consistent with that observed for other silicates.

$$D_{oxygen,\ \text{“dry”}} = 1.3\times10^{-4} exp(-448\ \text{kJ mol}^{-1}/RT)$$

Little anisotropy was noted in dry diffusion, as diffusion rates parallel and perpendicular to *c* were found to be quite similar. The diffusivities defined by this Arrhenius relation are consistent with the diffusivity at 1300°C obtained by Muehlenbachs and Kushiro (1975).

While most of the dry experiments conformed well to a complementary error function, which is the solution to the diffusion equation for the initial and boundary conditions imposed by the experiments, profiles from some of these dry experiments showed evidence of "tails," i.e., somewhat elevated (above natural abundance) ^{18}O concentrations extending to depths in the zircons up to twice the length of the error-function portion of the profile. The presence of the tails did not affect diffusivities calculated from the steep portion of the profile, since diffusivities from samples with and without tails yielded similar results when fitting this portion of the spectrum. The tails are most likely attributed to the presence of localized regions containing either fluid inclusions (which had not decrepitated in the 1300°C pretreatment of zircons before diffusion anneals) or oxygen defects.

Oxygen diffusion under "wet" conditions in significantly faster than "dry" diffusion, although D is insensitive to P_{H_2O} at values ≥7 MPa. The hydrothermal experiments run in the piston-cylinder show no indication of a dependence of oxygen diffusion on P_{H_2O} over the pressure range 0.4-1.0 GPa. Further, in experiments run with a 50:50 (molar) H_2O:CO_2 mix, so that $P_{H_2O} < P_{total}$, diffusivities obtained were indistinguishable statistically from cases where $P_{H_2O} = P_{total}$. The cold seal runs at lower pressures (7-70 MPa) have a mean value of log D about half a log unit lower than the mean value of log D for the higher-pressure experiments (Fig. 12). Although there is no systematic variation in D with pressure among the cold-seal runs, a slight dependence of D_{wet} on P_{H_2O} between ~70 and 400 MPa cannot be ruled out. While the possible weak dependence of D_{wet} on P_{H_2O} may introduce minor complication to Arrhenian behavior, the data for the wet experiments can nonetheless be considered generally consistent over the entire range of T and P, and therefore it is not wholly unreasonable to plot these data and fit to a single Arrhenius relation, which yields (Fig. 11):

$$D_{oxygen,\ \text{“wet”}} = 5.5\times10^{-12} exp(-210\ \text{kJ mol}^{-1}/RT)$$

The "wet" and "dry" Arrhenius relations indicate that oxygen diffusion in zircon is significantly enhanced by the presence of water in the system, in contrast to the behavior of Pb in zircon, for which diffusivities appear unaffected by the presence of hydrous species. Further, since the activation energy for diffusion of oxygen is much smaller under wet conditions than under dry (i.e., 210 vs. 448 kJ mol^{-1}), the difference between dry and wet diffusivities will increase with decreasing T (the variance will be, for example, about 6 orders of magnitude at 700°C). This sort of behavior, i.e., faster diffusivities and lower activation energies for oxygen diffusion under hydrothermal versus dry conditions, is common in silicates, including diopside (Ryerson and McKeegan 1994, Farver 1989), anorthite (Ryerson and McKeegan 1994, Giletti et al. 1978), sanidine (Freer et al. 1997, Derdau et al. 1998), and quartz (Dennis 1984, Giletti and Yund 1984). It is commonly argued (e.g., Farver and Yund 1990, 1991; Zhang et al. 1991, Doremus 1996) that molecular water is the dominant species transporting oxygen under hydrothermal conditions, and that the uncharged H_2O molecule moves move readily than highly-charged oxygen anions.

The weak (to nonexistent) dependence on f_{H_2O} for oxygen diffusion in zircon under hydrothermal conditions contrasts with trends observed for other minerals. Quartz (Farver and Yund 1991), calcite (Farver 1994) and alkali feldspar (Farver and Yund 1990) all exhibit increasing oxygen diffusivities with increasing f_{H_2O}. Assuming that fast-diffusing oxygens are carried by neutral water molecules (e.g., Zhang et al. 1991), it is perhaps the case that the closely-packed zircon structure becomes 'saturated' with water molecules at comparatively low water pressures, while the more open lattices of the other minerals can carry increasing amounts of water when water fugacities are increased.

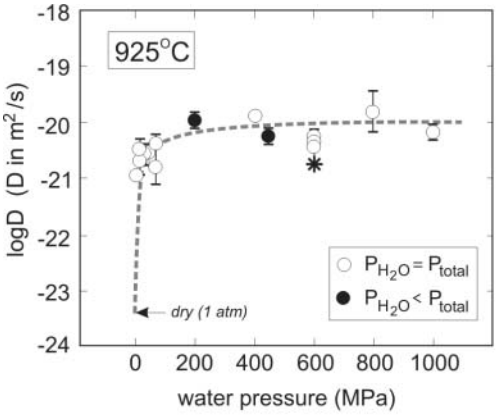

Figure 12. Oxygen diffusion as a function of water pressure at ~925°C. The cluster of points at $P_{H_2O} < 100$ MPa represents experiments made in cold-seal pressure vessels (two actually run at 917°C); all other symbols are for data obtained in piston-cylinder runs. The filled symbols show diffusivities resulting from experiments in which the fluid surrounding the zircon was a 50:50 (molar) H_2O:CO_2 mix; for these experiments, P_{total} is 400 and 800 MPa, respectively. The asterisk symbol represents a duplicate analysis, by ion microprobe (all others were done with nuclear reaction analysis), of one of the 600 MPa experiments. From the study of Watson and Cherniak (1997).

Diffusion mechanisms

As in the case of cations, we can look at theoretical calculations of energies of formation and migration of defects in zircon to explore possible mechanisms for oxygen diffusion. Williford et al. (1999) obtain oxygen vacancy migration energies ranging between 0.99-1.16 eV (95-110 kJ mol^{-1}), considerably smaller than activation energies for oxygen diffusion. Formation energies for oxygen vacancies are much higher: He and Cormack (1998) predict 3.31-6.52 eV/defect (320-630 kJ mol^{-1}). The experimentally determined activation energy for oxygen diffusion in zircon under dry conditions (448 kJ mol^{-1}; Watson and Cherniak 1997) falls within the range bracketed by the summed value of energies of formation and migration of oxygen vacancies. Crocombette (1999) estimates a value of 5.6 eV (540 kJ mol^{-1}) for formation energies of oxygen vacancies, but a much smaller value, 1.7 eV, for formation of oxygen interstitials. Migration energies for oxygen interstitials were not determined, but may be considerably higher than those for oxygen vacancies. Because of this uncertainty, an interstitial mechanism cannot be ruled out.

The presence of "tails" on some of the oxygen diffusion profiles measured by Watson and Cherniak (1997) (see also the section above) points to the possibility of two distinct diffusion mechanisms under some circumstances. It should be noted, however, that these features only appeared for a small number of the zircon specimens analyzed, and are not a dominant contributor to oxygen diffusion under dry conditions. Williford et al. (1999) and Watson and Cherniak (1997) argue that the tails may be a consequence of the presence of pre-existing oxygen vacancies in the zircon permitting a fast diffusion pathway with lower activation energy, those zircons more "vacancy deficient" would require a significant contribution to the activation energy from vacancy formation. However, this explanation would require that the fast diffusion pathway communicate poorly with the bulk structure. Otherwise, since individual atoms cannot distinguish between intrinsic and extrinsic vacancies, the profile would appear as a simple single error function rather than a "normal" diffusion profile superposed on an extended tail region akin to that observed for grain-boundary diffusion. A possible way around this dilemma is to invoke the presence of a localized region containing oxygen vacancies that is much smaller than the ~1mm^2 area of the proton beam used for ^{18}O analysis in NRA, but of significant extent in the direction of diffusion. The existence of such regions is not unreasonable given the complex internal chemical structure of the Mud Tank zircon as revealed, for example, by cathodoluminescence imaging. This model would also explain the sporadic occurrence of the tails in the oxygen diffusion profiles. An alternative explanation is that the fast oxygen transport path can be attributed to the presence of fluid inclusions (which had not decrepitated in the 1300°C pretreatment of zircons before diffusion anneals). Oxygen can likely migrate interstitially as a component of molecular H_2O, with transport facilitated by the fluid inclusions, and, as noted above, oxygen diffusion in the presence of water is considerably faster than under dry conditions.

IMPLICATIONS AND APPLICATIONS OF DIFFUSION FINDINGS

Diffusive fractionation

We now consider some potential consequences of differences in diffusion rates among the REEs and other cations. Could there be, for example, diffusional fractionation effects over geologically relevant time-temperature conditions? We first consider the Sm-Nd system. Using the expression above for variation of diffusion coefficients with REE ionic radii, diffusivities of Sm and Nd may differ by a factor of about 8 at 1000°C. This translates to diffusion distances differing by a factor of about 2.8 (i.e., diffusion distance $x \sim (Dt)^{1/2}$) for a given time at this elevated temperature. At 800°C, the difference in diffusivities would be over 2 orders of magnitude, but diffusivities are so small (i.e., 10^{-30} m^2sec^{-1}) as to be geologically irrelevant. Diffusion for a billion years at 800°C would result in diffusion distances on order of several nanometers at most. Even at 1000°C, diffusion distances would only amount to a few tens of microns over the same duration.

Diffusional fractionation does seem a more likely possibility for the Lu-Hf system. Hf diffuses 4-5 orders of magnitude more slowly than the REEs. A difference in diffusion rates of 4 orders of magnitude would lead to diffusion distances differing by a factor of ~100; at 1000°C this is equivalent to about 150 μm for Lu vs. < 2 μm for Hf over a billion years.

Closure temperatures

We can use experimentally-determined diffusion parameters to directly calculate closure temperatures (T_c) for various species in zircon as a function of effective diffusion radius and cooling rate, and these values can be compared with field based estimates for the closure temperatures for Pb. The closure temperature equation (Dodson 1973) is:

$$E/(RT_c) = \ln((ART_c^2D_o/a^2)/(EdT/dt)) \quad (2)$$

where E and D_o are the activation energy and pre-exponential factors for diffusion of the relevant species, dT/dt is the cooling rate, a is the effective diffusion radius, and A is a geometric factor. The derivation of the above expression rests on several assumptions (Dodson 1973, 1986); among these is the condition that at peak temperature T_o, the mineral grain is not retentive of the daughter product over short timescales. This assumption, which makes T_c independent of T_o, is, as Ganguly et al. (1998) note, not satisfied for slowly diffusing species. Given that cation diffusion in zircon appears to be exceedingly slow under crustal conditions, this condition is not satisfied nor can it even be assumed that homogeneity is achieved at peak metamorphic temperatures.

When the dependence of T_c on T_o is taken into account in calculating closure temperatures, the deviations of T_c from conventional closure temperatures calculated using Equation (2) are smaller with increasing peak temperature (T_o) and slower cooling rate (Ganguly et al. 1998). The geometric factor, A, in Dodson's expression of mean closure temperature above, is equal to $\exp(G)$, where G is the value of the closure function, $G(x)$, spatially averaged over the crystal. In deriving the expression for $G(x)$, and ultimately A, the dimensionless parameter M [where M is defined as $D(T_o)RT^2/(Ea^2dT/dt)$], is much greater than 1 (Dodson 1986). For smaller values of M, G will decrease, thus A will be smaller than the value of 55 [i.e., exp(4.0066)] one obtains when the condition of $M >> 1$ is met. As the factor A decreases, mean closure temperatures will be increased.

As noted above, closure temperatures calculated using Equation (2) are mean values, as closure temperature varies with distance from the crystal surface. However, except for a very narrow outermost layer, closure temperatures will not differ from the mean by more than a few tens of degrees for cooling rates between 1-10°C/Ma and grain sizes up to a few mm. For example, for 100-μm radius grains, mean T_c for Pb in zircon is about 10°C higher than that for a point 10 μm from the surface; T_c for the grain center will be about 40°C higher than the mean value. A point 1 μm from the surface, however, will have a T_c 80-90°C lower than the mean.

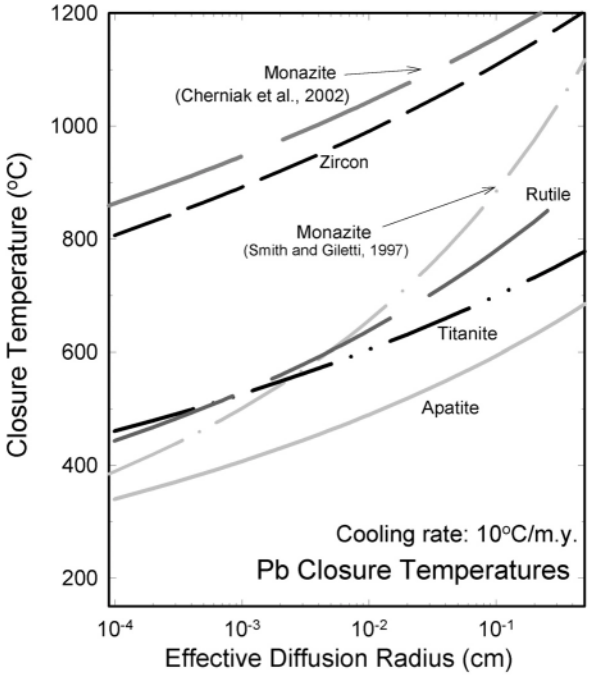

Figure 13. Closure temperatures for Pb in accessory minerals as function of effective diffusion radius for a cooling rate of 10°C per million years. Calculations were made employing the standard expression of Dodson (Eqn. 2). Sources for data: apatite - Cherniak et al. (1991); monazite - Smith and Giletti (1997); Cherniak et al. (2002); rutile - Cherniak (1998b); titanite - Cherniak (1993); zircon - Cherniak and Watson (2001). Closure temperatures Pb in zircon are quite high, considerably in excess of those for other accessory minerals except for monazite.

It should be clear from the above discussion that T_c is dependent on many factors. Nonetheless, we can use the simplified expression above to make broad comparisons of closure of Pb in various accessory minerals, and to consider closure temperature values calculated from the diffusion parameters presented earlier in this chapter in light of field-based estimates of closure temperatures for Pb in zircon.

In Figure 13 we plot closure temperature of Pb for various accessory minerals as function of effective diffusion radius, using the "traditional" Dodson equation (Eqn. 2). We plot curves calculated using the geometric factor for spherical geometry (i.e., $A = 55$). Closure temperatures for Pb in zircon are quite high, considerably in excess of those for other accessory minerals, with the exception of monazite (Cherniak et al. 2002). For example, the closure temperature for Pb in a zircon of 100 μm effective diffusion radius for a cooling rate of 10°C/Ma is 991°C. Evidence in field based studies of the high closure temperature (in excess of 950-1000°C) for Pb in zircon has long been noted (e.g., Black et al. 1986, Claoué-Long et al. 1991, Williams 1992). Higher closure temperatures for zircon in comparison to most other accessory minerals are evidenced by various studies (e.g., McLelland et al. 1988, Mezger et al. 1991, Chiarenzelli and McLelland 1993, Hölzl et al. 1994) that have observed, for example, that titanite from high grade metamorphic terranes yield U-Pb ages younger than zircons from the same samples, or other samples experiencing the same geologic history. Given the same cooling rate and effective diffusion radii (i.e., 10°C/Ma and 100 μm), calculated closure temperatures for titanite are 385°C lower than that of zircon. Both apatite and rutile have even lower closure temperatures, with only monazite displaying closure temperatures comparable to zircon.

The preservation of zoning in zircon

Sharp compositional zoning in zircon is often observed, as the slow diffusivities characteristic of most elements in zircon can influence both the likelihood of formation of such zoning (e.g., Watson and Liang 1995) and its preservation under a broad range of geologic conditions (Watson and Cherniak 1997, Cherniak et al. 1997a,b). Both sector zoning and igneous growth or "oscillatory" zoning have been reported in various zircon populations, with zoning down to micron and sub-micron scales (e.g., Hanchar and Miller 1993, Halden et al. 1992, Wayne et al. 1992, Corfu et al., this volume). Species for which zoning is most commonly noted are the high-Z elements incorporated into zircon in relatively high abundance (Hf, and to lesser extent, U), with zoning observ-

able in back-scattered electron (BSE) images, and the REE (most notably Dy), whose emissions often dominate the visible in cathodoluminescence (CL) spectra (e.g., Marfunin 1979, Mariano 1989).

While zoning in Pb generally cannot be observed by these means because of its low abundance and the fact that its electronic structure militates against its being a CL activator in zircon, marked variations in Pb isotopes across individual grains, representing different stages (and ages) of zircon growth, have been detected in ion probe analyses (e.g., Hanchar and Rudnick 1995, Ireland and Williams, this volume), and discordance in many cases has been attributed to "mixing" as consequence of combining isotope information from distinct regions into a single analysis.

Given the slow diffusion rates of Pb, REE, and the tetravalent cations in crystalline zircon under most geologic conditions, distinct zones, even on relatively fine scales, will quite often be preserved. This can be illustrated by a simple model. Zones in a zircon are modeled as plane sheets of thickness l; adjacent planes have different concentrations of diffusant. Only diffusion normal to the planar interface is considered. Two different (and somewhat arbitrary) criteria for alteration of zones are evaluated: (i) "blurring" of zones, defined by a compositional change of 10% one-tenth of the way into the zone; and (ii) "disappearance" of zones, defined by a compositional change of 10% in the zone's center. The dimensionless parameter Dt/l^2 is equal to 1.8×10^{-3} for condition (i), and 3.3×10^{-2} for condition (ii). Figure 14 shows curves constraining the time-temperature conditions

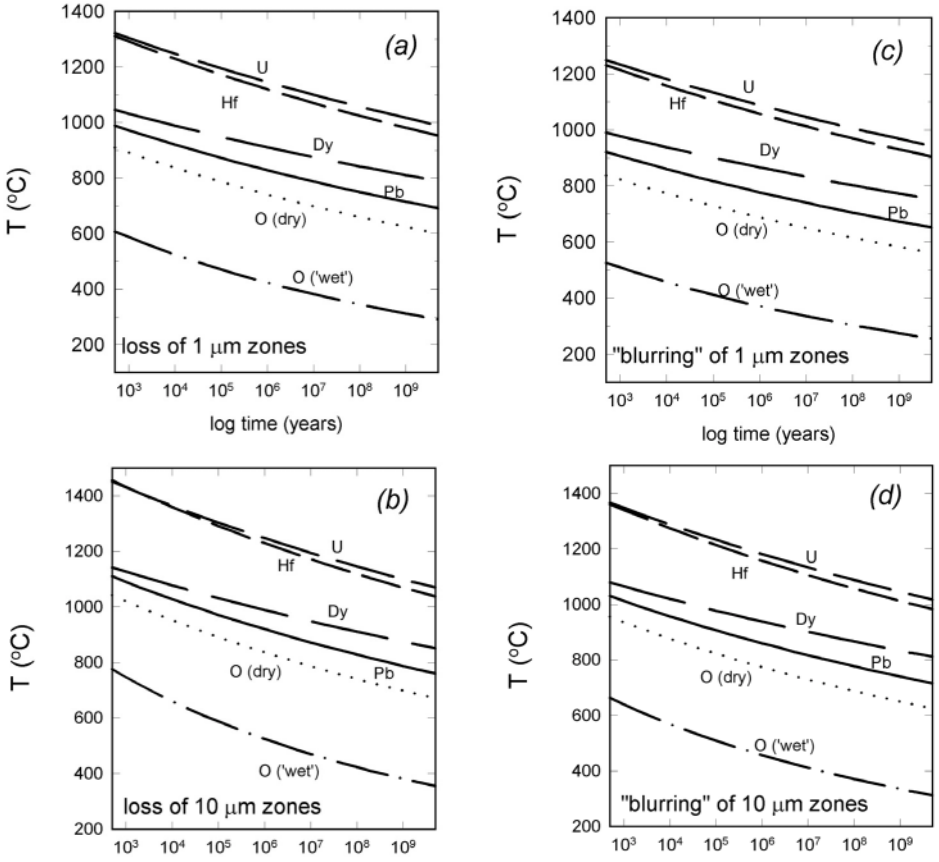

Figure 14. Preservation of cation and oxygen zoning in zircon. Curves represent maximum time-temperature conditions under which 1 and 10 μm zoning of U, Th, Dy, Pb and O (under dry and wet conditions) will be preserved in zircon. For conditions above the curves in a and b, well-defined zoning will be lost. For conditions above the curves in c and d, edges of zones will be "blurred" but still retain initial composition in zone centers.

under which Pb, REE, U, and Hf zoning of various dimensions will be retained given the above criteria. For example, 10-μm scale zones would resist obliteration at 750°C over times greater than the age of the Earth; even at 900°C, zones of this dimension would endure for a few million years.

Although the diffusion rates of Pb in zircon do not differ greatly from those of the REE over the investigated temperature range (Fig. 10), the differences in activation energy for diffusion (550 kJ mol^{-1} for Pb vs. 690-840 kJ mol^{-1} for the REE) result in significant differences in diffusion rates at most temperatures of geologic interest. For example, at 800°C, diffusion rates of Dy and Pb will differ by more than 2 orders of magnitude, with diffusion distances (which scale as the square root of D) differing by a factor of ~20. Differences become even more pronounced with decreasing temperature. Hence, the preservation of REE zoning observable with CL spectroscopy does not guarantee preservation of Pb isotope signatures on the same scale, as can be seen from the set of curves for Dy zoning also plotted in Figure 14. Preservation of BSE-observable zoning in Hf or U offers even less evidence for simultaneous preservation of Pb zoning, as diffusion of the tetravalent cations is considerably slower than that of the REE (Cherniak et al. 1997b).

Similarly, the preservation of Pb isotope ratios in no way guarantees that oxygen isotopes from the same region of zircon are preserved, given the large differences in Pb and oxygen diffusivities, even under dry conditions (Fig. 10). For example, zoning on the 10 μm scale would be preserved for Pb over nearly 100 Ma at 900°C; for oxygen these time would be 100,000 years and only a few decades for dry and wet conditions, respectively (Fig. 14).

It should be made clear, however, that these diffusion data apply strictly to crystalline zircon. Diffusion may be significantly enhanced in severely radiation-damaged zircon (e.g., Cherniak et al. 1991), thus permitting the obliteration of zoning under much less extreme thermal conditions. Further discussion of the influence of radiation damage, and other factors, on Pb transport will be taken up in the next section.

Pb loss

Discordant U-Pb ages are on occasion attributed, generically, to "Pb loss" (Parrish et al., this volume; Davis et al., this volume). Laboratory diffusion measurements indicate that Pb diffusion in crystalline zircon is remarkably slow, thus it is highly unlikely that significant amounts of Pb will be lost from crystalline zircon at geologically reasonable temperatures due to volume diffusion. Figure 15 illustrates this point. The curves represent the percent of Pb loss for zircons of 10- and 100-μm radii when subjected to various time-temperature conditions. Zircon crystals of 10-μm radius would lose only about 1% of their Pb if residing at 750°C for times on order of the age of the Earth. Zircons exposed to upper mantle temperatures for extended periods of time would, however, experience significant Pb loss through diffusion, although not always complete resetting, as suggested by studies of kimberlitic zircons (Scharer et al. 1992, Mezger and Krogstad 1997).

Pb loss due to diffusion is more likely in metamict zircons, since Pb diffusion has been found to be much more rapid in zircon that has been severely radiation-damaged (Cherniak et al. 1991). Radiation damage, however, takes significant amounts of time to accumulate because of the natural annealing that occurs on geologic timescales (e.g., Lumpkin and Ewing 1988, Meldrum et al. 1998). The annealing process is such that zircons residing at temperatures above a "critical amorphization temperature" will not become metamict. The critical amorphization temperature is a weak function of activity, i.e., zircon U content and age (Meldrum et al. 1998). The critical amorphization temperature for zircons with 1000 ppm U is about 360°C, and only about 20°C higher for zircons with as much as 10,000 ppm (i.e., 1%) uranium; it varies as a function of zircon age by less than a degree per billion years for a given U content. Zircon crystals exposed to temperatures below the critical amorphization temperature can accumulate damage, but only over long time scales.

Using the expressions derived by Meldrum et al. (1998), curves can be generated defining the range of time-temperature conditions that radiation damage in zircon will accumulate to sufficient degree that the zircon becomes metamict. This curve is plotted in Figure 15. It can be readily noted

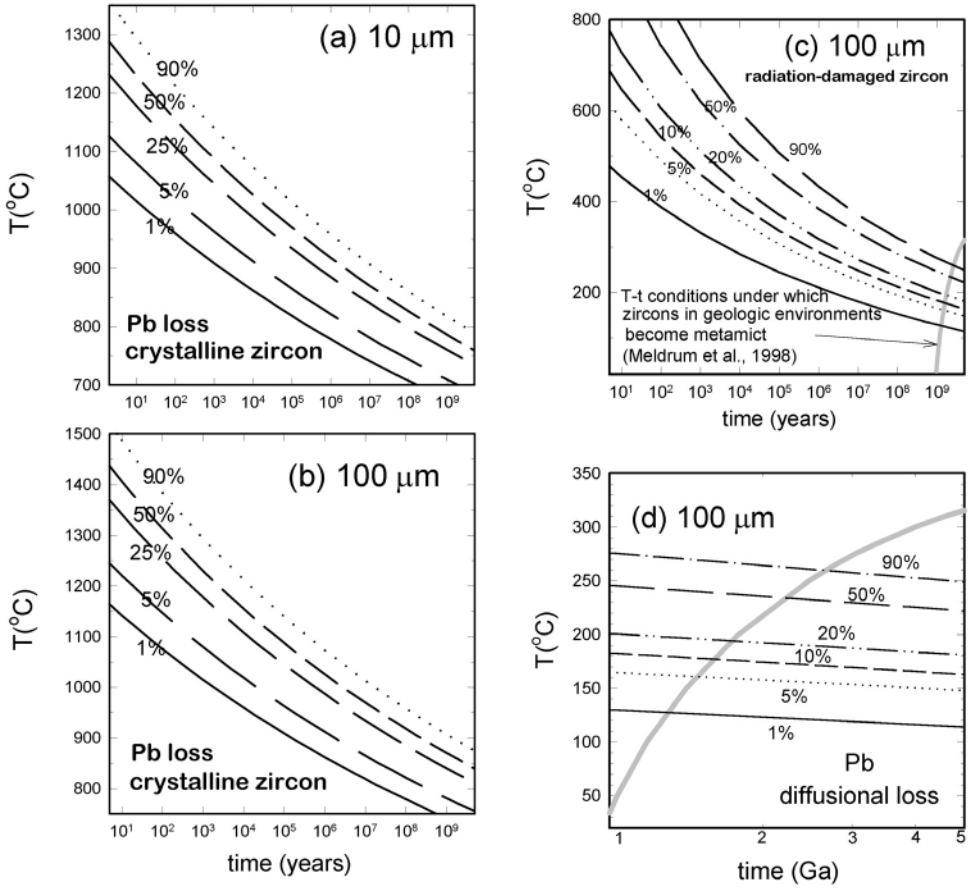

Figure 15. (a) and (b) Conditions for diffusional Pb loss in crystalline zircon for zircons of effective radii of 10 and 100 μm. Curves represent time-temperature conditions under which zircon will lose the indicated fraction of total Pb, calculated using the diffusion parameters from Cherniak and Watson (2001). (c) and (d) Conditions for diffusional Pb loss in metamict zircon. Curves represent time-temperature conditions under which a zircon of 100 μm radius will lose the indicated fraction of Pb. These are generated using the diffusion data of Cherniak et al. (1991) for radiation-damaged zircon. Also plotted is a curve indicating time-temperature conditions under zircon with 100 ppm U will become metamict, calculated from the expressions in Meldrum et al. (1998). Times in excess of a billion years, even at near-surface temperatures, are necessary in order for the zircon to accumulate sufficient radiation damage to become metamict. Significant Pb loss will be likely only in the region below this curve.

that times upward of a billion years at low temperatures are required to induce amorphization, and, as noted above, damage sufficient to cause amorphization will fail to accumulate at elevated temperatures. Also plotted against this curve are curves indicating the degree of diffusional Pb loss for metamict zircon. The diffusion data of Cherniak et al. (1991) are used here, since the zircons are considered severely radiation-damaged under these circumstances. Added complexities, such as the possibility that Pb transport rates may change with differing degrees of radiation damage, and the two-stage annealing kinetics of zircon (e.g., Weber et al. 1994, Meldrum et al. 1998) were not considered in this simple model. In severely radiation-damaged zircon, in contrast to crystalline zircon, significant amounts of diffusional Pb loss are possible, even at relatively low temperatures given the enhanced transport rates in the damaged material. Complete resetting of Pb isotopes through volume diffusion could also occur if zircon possessing significant amounts of radiation damage (in residing at low temperatures) were rapidly heated, since the zircon structure is slow to recover

crystallinity after experiencing radiation damage beyond certain levels (e.g., Weber et al. 1994, Murakami et al. 1991, Weber 1990), and Pb diffusion would remain relatively rapid.

It has long been argued (e.g., Silver and Deutsch 1963) that there exists a correlation between U content and discordance, although there are cases (e.g., Schärer and Allègre 1982) where this relationship does not seem to apply. Recent work (Sanborn et al. 1998, Stern et al. 1998), however, continues to point to the complexity of the phenomenon of "Pb loss" in natural zircon. While some correlation between U content and degree of discordance in mildly discordant (<10%) zircons studied has been found, suggesting a possible role of enhanced volume diffusion in radiation damaged zircon, there is often no such correlation in severely discordant zircon, indicating possible influence of other (non-diffusional) processes, such as recrystallization and various fluid-assisted processes, including physical deformation (e.g., Pidgeon et al. 1998, Sinha et al. 1992), that could significantly alter Pb isotope ratios and zircon U contents. The zircon composition itself can be an important factor influencing the probability of recrystallization. Pidgeon et al. (1998) argue that recrystallization (and consequent exclusion of trace elements from the zircon structure) is more likely in zircon (or regions of zircon) with high trace element concentrations, as the zircon crystal, experiencing strain due to the significant substitution of these other elements, can become metastable upon cooling from magmatic temperatures.

Preservation of oxygen isotope signatures

It is now possible to measure oxygen isotopic ratios in minerals *in situ* (e.g., Valley et al. 1994, 1998; Sharp 1992, Elsenheimer and Valley 1993, Reeder et al. 1997, Wiechert et al. 2002, Valley, this volume), and it is likely that techniques will continue to be refined and find broader application. The capability of measuring isotopic profiles within single mineral grains may, in conjunction with experimentally acquired data on oxygen diffusion and isotopic fractionation among minerals, permit the extraction of information on the thermal history of host rocks.

Time-temperature information can be obtained from measured diffusion profiles in a mineral by applying analytical or numerical solutions to the non-steady state diffusion equation, given relatively simple grain geometries and constrained initial conditions (e.g., Crank 1975). A small complication arises in applying these solutions in isotope geochemistry. 'Standard' diffusion equations describe changes in time and space of absolute concentrations of a diffusant, However, the quantities measured in natural samples are isotope ratios, but what are actually moving through the mineral structure are the atoms of ^{18}O and ^{16}O themselves, not the isotopic ratio. A simple case illustrates this point. Consider a one-dimensional, isothermal diffusive exchange between the near-surface region of a zircon and an infinite reservoir in which concentrations of both ^{18}O and ^{16}O are constant for the time interval concerned (e.g., a case with a contacting metamorphic fluid). The concentration of ^{18}O in the zircon as a function of time (t) and distance (x) is described by:

$$C_{18} = C_{18,i} + (C_{18,o} - C_{18,i})\ erfc(x/(4Dt)^{1/2}) \quad (3)$$

and similarly, the concentration of ^{16}O by:

$$C_{16} = C_{16,i} + (C_{16,o} - C_{16,i})\ erfc(x/(4Dt)^{1/2}) \quad (4)$$

where C_{18} and C_{16} are the concentrations of the isotopes at a distance x from the zircon-reservoir interface, and the subscripts i and o refer to the initial and surface concentrations of the isotopes in the zircon. It is assumed that both isotopes share the same diffusivity (D). Because the total amount of oxygen in the zircon is fixed by stoichiometry, there is the additional constraint in this case:

$$C_{18} + C_{16} = C_{18,o} + C_{16,o} = C_{tot} \quad (5)$$

where C_{tot} is a constant. [This last constraint would not apply to most isotope systems. For example, the total amount of Sr in a plagioclase feldspar need not be fixed at a constant value, as Sr could exchange for Ca, so ^{87}Sr and ^{86}Sr could vary.] Equations (3) and (4) make it clear that the quantity actually profiled in a mineral grain (i.e., C_{18}/C_{16}) would vary with depth in a sample not as a simple error function but as the ratio of two quantities described by two distinct error function relationships (e.g., Zhang et al. 1991). However, given the relative abundances of ^{18}O and ^{16}O found in nature (~0.2% and ~99.8%), the value of $^{18}O/^{16}O$ as a function of t and x does in fact closely conform to an error function because the numerator is effectively constant. Consequently, $^{18}O/^{16}O$ can be thought of as the diffusant, and measured gradients in the isotope ratio can be accurately modeled using standard solutions to the diffusion equation.

Some controversy exists concerning whether the Arrhenius relations for 'dry' or 'wet' oxygen diffusion should be applied to particular systems (e.g., Kohn 1999, Valley et al. 2002, Peck et al. 1999, 2001; Wilde and Valley 2001). Most applications of the zircon data will likely be to igneous and metamorphic events in the Earth's crust. Since the transition from 'dry' to 'wet' diffusion behavior appears to be essentially complete at $P_{H_2O} \approx 6.9$ MPa, the 'wet' Arrhenius relation is probably appropriate for most crustal processes. Oxygen diffusion in zircons participating in crustal igneous events is likely to be 'wet' merely because melting in the crust is generally predicated upon the presence of water. Oxygen diffusion in zircons from metamorphic systems containing a fluid phase and/or hydrous minerals is also probably well described by the 'wet' diffusivites. Kohn (1999) notes that most metamorphic rocks have mineral assemblages that can buffer f_{H_2O} during cooling, and that although a rock may be 'dry' in the sense of lacking a fluid phase it may still be 'wet' in the thermodynamic sense that f_{H_2O} is much greater than 1 bar. The only natural zircons, then, to which the 'dry' diffusion results appear applicable would be those from granulite facies rocks, from dry regions of the mantle, or from extraterrestrial samples. This conclusion seems inevitable provided that H_2O fugacity (with fluid absent) has the same effect on oxygen diffusion as does H_2O pressure (with fluid present). This proviso seems thermodynamically reasonable, but has not been confirmed by experiment.

$^{18}O/^{16}O$ retention in zircon cores and rims

In situ determination of oxygen isotope ratios in natural materials can now be carried out on ~20-μm spots with an accuracy of ~0.5 $\delta^{18}O$ units (e.g., Valley et al. 1997), making it possible to investigate the internal oxygen isotope structure of minerals with the aim of deciphering complex crystallization and/or thermal histories. It is therefore useful to explore the systematics of retention of oxygen isotopic ratios in local regions of individual grains.

It is well known that zircon crystals often contain a record of multiple crystallization events that may be revealed by CL or BSE imaging (e.g., Hanchar and Miller 1993, Hanchar and Rudnick 1995, Vavra et al. 1996, Corfu et al., this volume). In the simplest case, complex histories are manifested by an 'old' core mantled by a 'young' rim. Given the typically small size of crustal zircons (~50-200 μm) it may not be possible to characterize intra-grain $^{18}O/^{16}O$ gradients in detail, but measurements of isotope ratios in the central regions of grain cores and rims—where the original isotopic signatures of these features are most likely to be preserved—is an attainable goal. The question when approaching analyses of these features concerns what time-temperature conditions will preserve the original $^{18}O/^{16}O$ signature in the central region of the feature of interest. The average (bulk) $\delta^{18}O$ value of a core or rim may be modified considerably by diffusion, but as long as the center of a specific feature is unaffected by diffusive exchange, key information related to the environment of crystallization may be retained.

For cases of isothermal annealing, calculation of time-temperature conditions for "center preservation" is straightforward because the diffusivity is independent of time, allowing the use of standard solutions to the non-steady state diffusion equation. For diffusion in a sphere, which could represent either a spherical zircon grain or a core within a larger zircon, the center will retain the

original $^{18}O/^{16}O$ for values of Dt/a^2 of up to 0.03, assuming that the oxygen isotope ratio remains constant at the sphere surface over the annealing interval (Crank 1975, p. 92). For a rim or mantle, the maximum time for center preservation differs from that of a sphere of the same radius because diffusion occurs radially both inward and outward. Given constant $^{18}O/^{16}O$ ratios at both the internal and external bounding surfaces, the analytical solution for a "hollow sphere" can be employed (Crank 1975, p. 98). The constant- surface condition is not strictly met at the inner boundary (due to radial diffusion effects), but it nearly holds for the range of core/rim dimensions of interest, so the solution of Crank (1975) can be used with more than adequate accuracy. [This was confirmed by detailed numerical of core-rim interdiffusion modeling in which the concentration at the internal bounding surface was allowed to vary (Watson and Cherniak 1997).] The maximum time for preservation of the original $^{18}O/^{16}O$ at the center of an overgrowth zircon rim is given by $Dt/x^2 \approx 0.012$, where x is the thickness of the rim.

Figure 16 illustrates the conditions of annealing time and temperature corresponding to the center-retention criteria stated above for $^{18}O/^{16}O$ in zircon cores ($Dt/a^2 = 0.03$) and rims ($Dt/x^2 = 0.012$). Calculations in Figure 16a are shown for 'wet' systems only, because they are thought to be most applicable to the Earth's crust. At an extreme lower crustal temperature of 900°C, center isotope retention is brief; only 160 or 5700 years, respectively, for cores of 20 and 120 μm. For overgrowth rims, time frames are even shorter: 16 to 570 years for rim thicknesses of 10 and 60 μm. In contrast, at a mid-crustal metamorphic temperature of 500°C, center retention times become geologically significant: 10^7 to 4×10^8 years for 20- to 120-μm cores, and 10^6 to 4×10^7 years for 10- to 60-μm rims. The conditions shown in Figure 16 should serve as a useful guide for evaluation of $^{18}O/^{16}O$ spot analyses made in the central regions of zircon cores and rims revealed by CL or BSE

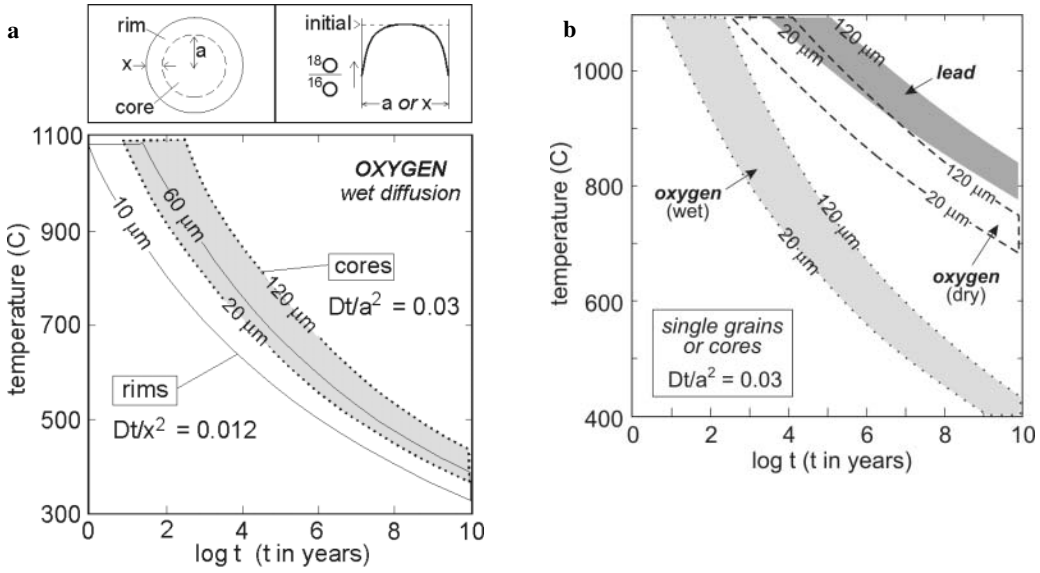

Figure 16. (a) Oxygen isotope center-retention criteria for isothermal annealing of zircon cores and rims under wet conditions, using the diffusion data from Watson and Cherniak (1997). The curves define the maximum annealing duration that a spherical core of rim can experience at a particular temperature and still retain the original $\delta^{18}O$ at its center (see diagram at upper right). These maximum times are defined by critical values for Dt/a^2 or Dt/x^2 (where a is core radius and x is rim thickness) of 0.03 and 0.012, respectively. (b) Curves comparing center-retention criteria for oxygen under wet and dry conditions (Watson and Cherniak 1997), and Pb (Cherniak and Watson 2001). In this figure, only curves for retention in cores (or single grains) of 20 and 120 μm are plotted. Zircon is significantly more retentive of Pb than oxygen isotopes, even for oxygen diffusion under dry conditions.

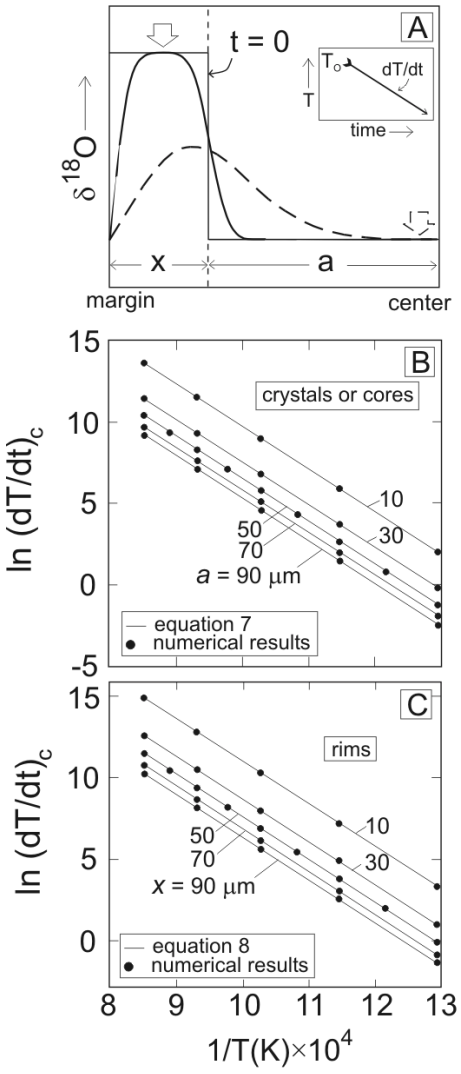

Figure 17. Oxygen diffusion center-retention criteria for spherical zircon cores and rims cooling under wet conditions (Watson and Cherniak 1997). The schematic diagram in (a) shows a radial profile of $\delta^{18}O$ (initially a step distribution) which relaxes toward homogeneity with increasing time at high temperature. There is a critical cooling rate - $(dT/dt)_C$, assumed here to be linear—below which the original $\delta^{18}O$ value at the center of a core or rim will fail to be preserved. If cooling is too slow, $\delta^{18}O$ will detach from the original core or rim value. The thicker lines show the $\delta^{18}O$ profile just prior to detachment at the center of the rim (solid line) and of the core (dashed line). The diagram implies a $\delta^{18}O$ for the surrounding medium equivalent to that of the core but the model results shown in (b) and (c) are independent of the relative $\delta^{18}O$ values of the core, rim and host medium. (b) and (c) Results of numerical simulation of wet oxygen diffusion to determine the critical minimum cooling rate, $(dT/dt)_C$, for retention of the original $\delta^{18}O$ value at the center of a spherical zircon crystal or core (b), or rim (c). The dots represent the actual numerical results; the lines are fits to the numberical data given by Eqs. (7) and (8). See text for additional discussion.

imaging. However, it should be stressed that diffusivities of the middle REE (the predominant activators of CL in zircon) and especially the tetravalent cations Hf and U (elements often responsible for zoning visible in BSE imaging) are considerably slower than diffusion rates for oxygen, so the zoning in these elements may be preserved well after distinct oxygen isotope signatures are lost through diffusional exchange. Also important to consider when interpreting oxygen isotope signatures from zircons for which U/Pb isotope ages are also obtained is the relative retentivity of Pb vs. oxygen isotopes in zircon. Curves for Pb, using the same center-retention criteria above, are plotted in Figure 16b along with those for oxygen. It is clear that zircons will be much less retentive of oxygen isotope signatures than Pb, so great care must be taken when attempting to correlate oxygen isotope ratios with U/Pb ages.

At present, the principal limitation to the usefulness of such analyses may well be the lack of information on oxygen isotope fractionation between zircon and other phases. The main shortcoming of the results shown in Figure 16 is that (for lack of a better choice) we assumed an initial 'step' distribution in $^{18}O/^{16}O$; that is, an abrupt discontinuity at the core/rim boundary. In many instances, zircon growth is likely to be slow in relation to oxygen diffusion, so an isotopic discontinuity, if preserved at all, may be 'blurred' substantially by diffusion during growth of the rim. This disclaimer may be especially important for igneous overgrowth situations, where the temperatures are high (thus promoting oxygen isotopic equilibration), and growth is slow because it is limited by Zr diffusion in the melt.

Retention at rim and core centers during cooling

Having treated bulk $^{18}O/^{16}O$ in a cooling regime, as well as local retention during isothermal annealing, we turn now to the question of retention in central regions of zircon cores and rims during cooling. The problem was addressed from a somewhat different angle by Dodson (1986), who provided the mathematical basis for calculating closure profiles (i.e., closure temperature vs. radial position) within mineral grains. Oxygen isotopes do not provide information on mineral age, so we posed the closure question in a different way: How fast must a zircon cool in order to preserve at its center the $^{18}O/^{16}O$ ratio acquired at the time of its growth? This question seems important if $\delta^{18}O$ values are to be used to deduce zircon provenance.

For the sake of completeness, we consider as before a hypothetical "mantled" zircon. At some initial temperature (T_o), the core and rim and isotopically distinct, with $^{18}O/^{16}O$ changing abruptly at the interface (Fig. 17). If cooling from T_o is slow, the oxygen isotopes will interdiffuse, possibly obliterating the original core and rim signatures. On the other hand, if cooling is fast, memory of the original ratios may be retained in the central region of the core and/or rim. As previously noted, the assumption of an initially abrupt discontinuity in $^{18}O/^{16}O$ at the core/rim interface (Fig. 17) is unrealistic for many circumstances, especially if T_o is of lower crust magnitude. There may be few cases where $^{18}O/^{16}O$ retention in rim features is relevant to cooling scenarios such as those considered. The core retention results, however, do have general relevance because the conclusions apply to any crystal or region of a crystal having a broadly spherical shape.

The initial step distribution shown in Figure 17 was used as a starting point to model $^{18}O/^{16}O$ interdiffusion during cooling from initial temperatures ranging between 400°C and 900°C. Both intracrystalline exchange (i.e., core-rim interdiffusion) and exchange with the zircon host medium are assumed to occur. A standard explicit finite-difference approach was adapted to a spherical geometry as described by Crank (1975, Chapter 8), using mass-centered volume elements. Additional details of the procedure are outlined in Watson and Cherniak (1997).

The most salient aspect of the numerical simulation is that the minimum (critical) cooling rate $(dT/dt)_c$ needed to preserve $^{18}O/^{16}O$ at the center of a spherical crystal or core is perfectly log-linear in T_o^{-1} (where T_o is the initial temperature in Kelvin):

$$\ln (dT/dt)_c = -27076/T_o + \text{const} \quad (6)$$

The same form of relationship applies to preservation of the initial ratio at the centers of overgrowth rims, and in both cases the constant is a simple function of the core radius (a) or rim thickness (x). Accordingly, the numerical results lead to simple equations that accurately describe the minimum cooling rates need to just preserve $^{18}O/^{16}O$ values inherited at high temperature:

$$\ln (dT/dt)_c = -27076/T_o - 2.041 \ln a + 41.9 \quad \text{(for crystals or cores)} \quad (7)$$

$$\ln (dT/dt)_c = -27076/T_o - 2.12 \ln x + 43.2 \quad \text{(for rims)} \quad (8)$$

where a and x are in microns, and dT/dt is expressed as °C/Ma. The relationships defined by Equations (7) and (8) are illustrated in Figure 17, which shows the near-perfect agreement between the actual numerical simulations (dots) and these generalized equations. An example calculation: Assume that a zircon in the lower crust (at, say, 650°C) has just grown a new 30-µm rim on a preexisting 70-µm core, and that the rim and core are characterized by distinct oxygen isotopic ratios. Equations (7) and (8) reveal that the zircon would have to cool at a rate of at least 49°C/Ma to preserve the $\delta^{18}O$ value at the center of the core, and at least 776°C/Ma to preserve $\delta^{18}O$ at the center of the rim.

At first glance, the above calculation would appear to call into question the conclusions (e.g., Valley et al. 1994, Peck et al. 1999) concerning the high $\delta^{18}O$ retentivity of Adirondack zircons. It is

important to bear in mind, however, that the diffusivity of oxygen must drop dramatically at f_{H2O} somewhat below 7 MPa. Because f_{H_2O} during retrograde metamorphism of high-grade rocks is poorly constrained (and may even vary locally within a given rock unit) it is not unreasonable to expect variability in isotopic closure of individual zircon crystals—caused, perhaps, by 'dry' diffusion behavior in some grains. However, as earlier noted, a rock may be 'dry' in the sense of lacking a fluid phase but may still be 'wet' in the thermodynamic sense that f_{H_2O} is much greater than 1 bar, and it remains unclear exactly at what values of f_{H_2O} the transition between 'wet' and 'dry' diffusion regimes occurs.

FUTURE DIRECTIONS

A large body of diffusion data exists for zircon, as this chapter has shown, but there are many directions for future research. One area of interest is diffusion of the noble gases, most notably He given its potential in low temperature thermochronometry (e.g., Reiners et al. 2002).

Also of interest are diffusion rates of other highly charged cations, including Nb and Ta, whose abundance and relative proportions have potential use in distinguishing zircons from various sources (e.g., Belousova et al. 2002), and which may also play a role in coupled substitutions involving other geochemically significant cation species (e.g., $(Nb, Ta)^{+5} + REE^{+3} \rightarrow 2\ Zr^{+4}$).

As mentioned in the previous section, there remains the issue of exploring fluid-absent but still thermodynamically 'wet' systems (i.e., with $f_{H_2O} > 1$ bar but less than 7 MPa) such as those with hydrous mineral phases present but no free water. This will permit a better understanding of the transition between 'wet' and 'dry' diffusion behaviors for oxygen diffusion in zircon, which may be of considerable importance in interpreting oxygen isotope measurements in natural systems.

The effects of radiation damage on diffusion are still to be systematically investigated. For Pb diffusion, there exist measurements of the "end member" cases: severely radiation-damaged zircon (Cherniak et al. 1991) and fully crystalline zircon (Cherniak and Watson 2001). It is not clear how intermediate amounts of radiation damage in the zircon structure would affect diffusivities. However, the fact that there are two simultaneously occurring kinetic processes (i.e., atomic diffusion and repair of the damaged zircon lattice) with potentially quite different activation energies and rates, complicates characterization of diffusivities (not to mention degree of radiation damage) under these circumstances.

ACKNOWLEDGMENTS

We thank Jim Van Orman and Rick Ryerson for their thorough reviews of the manuscript. Thanks also to John Hanchar for his editorial efforts, and to him and Paul Hoskin for their work on this volume and in organizing the short course from which it resulted. This work was supported by grants EAR-9527014 and EAR-0073752 from the National Science Foundation (to E.B. Watson).

REFERENCES

Belousova EA, Griffin WL, O'Reilly SY, Fisher NI (2002) Igneous zircon: trace element composition as an indicator of source rock type. Contrib Mineral Petrol 143:602-622

Black LP, Williams IS, Compston W (1986) Four zircon ages from one rock: the history of a 3939 Ma-old granulite from Mt. Sones, Enderby Land, Antarctica. Contrib Mineral Petrol 94:427-437

Bogolomov YS (1991) Migration of lead in non-metamict zircon. Earth Planet Sci Lett 107:625-633

Caruba R, Turco G, Iacconi P, Keller P (1974) Solution solide d'elements de transition trivalents dans le zircon et l'oxyde de zirconium, etude par thermoluminescence artificelle. Bull Soc Fr Minéral Cristallogr 97:278-283

Chapman HJ, Roddick JC (1994) Kinetics of Pb release during the zircon evaporation technique. Earth Planet Sci Lett 121:601-611

Cherniak DJ (2002a) Ba diffusion in feldspar. Geochim Cosmochim Acta 66:1641-1650

Cherniak DJ (2002b) REE diffusion in feldspar. Chem Geol 193:25-41

Cherniak DJ (2000) Rare earth element diffusion in apatite. Geochim Cosmochim Acta 64:3871-3885

Cherniak DJ (1998a) Rare earth element and gallium diffusion in yttrium aluminum garnet. Phys Chem Minerals 26:156-163

Cherniak DJ (1998b) REE Diffusion in calcite. Earth Planet Sci Lett 160:273-287

Cherniak DJ (1996) Strontium diffusion in sanidine and albite, and general comments on Sr diffusion in alkali feldspars. Geochim Cosmochim Acta 60:5037-5043
Cherniak DJ (1995) Diffusion of lead in plagioclase and K-feldspar: an investigation using Rutherford Backscattering and resonant nuclear reaction analysis. Contrib Mineral Petrol 120:358-371
Cherniak DJ (1993) Lead diffusion in titanite and preliminary results of the effects of radiation damage on Pb transport. Chem Geol 110:177-194
Cherniak DJ, Watson EB (2001) Pb Diffusion in zircon. Chem Geol 172:5-24
Cherniak DJ, Watson EB (1994) A study of strontium diffusion in plagioclase using Rutherford Backscattering Spectroscopy. Geochim Cosmochim Acta 58:5179-5190
Cherniak DJ, Watson EB (1992) A study of strontium diffusion in K-feldspar, Na-K feldspar and anorthite using Rutherford Backscattering Spectroscopy. Earth Planet Sci Lett 113:411-425
Cherniak DJ, Zhang XY, Wayne NK, Watson EB (2001) Sr, Y and REE diffusion in fluorite. Chem Geol 181:99-111
Cherniak DJ, Hanchar JM, Watson EB (1997a) Rare-Earth diffusion in zircon. Chem Geol 134:289-301
Cherniak DJ, Hanchar JM, Watson EB (1997b) Diffusion of tetravalent cations in zircon. Contrib Mineral Petrol 127:383-390
Cherniak DJ, Lanford WA, Ryerson FJ (1991) Lead diffusion in apatite and zircon using ion implantation and Rutherford Backscattering techniques. Geochim Cosmochim Acta 55:1663-1673
Cherniak DJ, Watson EB, Harrison TM, Grove M (2002) Pb diffusion in monazite. Geol Soc Am Ann Mtg, paper #138-5
Chiarenzelli JR, McLelland JM (1993) Granulite facies metamorphism, paleoisotherms and disturbance of the U-Pb systematics of zircon in anorogenic plutonic rocks from the Adirondack highlands. J Metamor Geol 11:59-70
Claoué-Long JC, Sobolev NN, Shatsky VS, Sobolev AV (1991) Zircon response to diamond-pressure metamorphism in the Kokchetav Massif, USSR. Geology 95:87-105
Crank J (1975) The Mathematics of Diffusion (2nd edn). Oxford Univ Press, Oxford, UK, 414 p
Crocombette JP (1999) Theoretical study of point defects in crystalline zircon. Phys Chem Minerals 27:138-143
Dennis PF (1984) Oxygen self-diffusion in quartz under hydrothermal conditions. J Geophys Res B 89:4047-4057
Derdau D, Freer R, Wright K (1998) Oxygen diffusion in anhydrous sanidine feldspar. Contrib Mineral Petrol 133:199-204
Dodson MH (1973) Closure temperature in cooling geochronological and petrological systems. Contrib Mineral Petrol 40:259-274
Dodson MH (1986) Closure profiles in cooling systems. Mater Sci Forum 7:145-154
Doremus RH (1996) Diffusion of oxygen in silica glass. J Electrochem Soc 143:1992-1995.
Dowty E (1980) Crystal-chemical factors affecting the mobility of ions in minerals. Am Mineral 65:174-182
Elsenheimer D, Valley JW (1993) Submillimeter scale zonation of $\delta^{18}O$ in quartz and feldspar, Isle of Skye, Scotland. Geochim Cosmochim Acta 57:3669-3676
Farver JR (1994) Oxygen self-diffusion in calcite: dependence on temperature and water fugacity. Earth Planet Sci Lett 121:575-587
Farver JR (1989) Oxygen self-diffusion in diopside with application to cooling rate determinations. Earth Planet Sci Lett 92:386-396
Farver JR, Yund RA (1991) Oxygen diffusion in quartz: dependence on temperature and water fugacity. Chem Geol 90:55-70
Farver JR, Yund RA (1990) The effect of hydrogen, oxygen, and water fugacity on oxygen diffusion in alkali feldspar. Geochim Cosmochim Acta 54:2953-2964
Foland KA (1974) Alkali diffusion in orthoclase. *In* Geochemical Transport and Kinetics. Hofmann AW, Giletti BJ, Yoder Jr HS, Yund RA, (eds) Carnegie Institution of Washington, Washington,DC, p 77-98
Fortier SM, Giletti BJ (1989) An empirical model for predicting diffusion coefficients in silicate minerals. Science 245:1481-1484
Freer R, Wright K, Kroll H, Göttlicher J (1997) Oxygen diffusion in sanidine feldspars and a critical appraisal of oxygen-isotope mass-effect measurements in non-cubic materials. Philos Mag A 75:485-503
Ganguly J, Tirone M, Hervig RL (1998) Diffusion kinetics of samarium and neodymium in garnet, and a method for determining cooling rates of rocks. Science 281 805-807
Gasparini P, Mantovani MSM, Ribiero FB (1984) Temperature dependence of radon diffusion from some rocks and minerals. Bollettino di Geofisica Teorica ed Applicata XXVI:135-141
Giletti BJ, Shanahan TM (1997) Alkali diffusion in plagioclase feldspar. Chem Geol 139:3-20
Giletti BJ, Casserly JED (1994) Strontium diffusion kinetics in plagioclase feldspars. Geochim Cosmochim Acta 58:3785-3793
Giletti BJ, Yund RA (1984) Oxygen diffusion in quartz. Chemical effects of water on the strength and deformation of crustal rocks. J Geophys Res B 89: 4039-4046
Giletti BJ, Semet MP, Yund RA (1978) Studies in diffusion: III, Oxygen and feldspars, an ion microprobe determination. Geochim Cosmochim Acta 42:45-57
Halden NM, Hawthorne FC, Campbell JL, Teesdale WJ, Maxwell JA, Higuchi D (1993) Chemical characterization

of oscillatory zoning and overgrowths in zircon using 3 MeV μm-PIXE. Can Mineral 31:637-647
Hanchar J M, Rudnick RL (1995) Revealing hidden structures: the application of cathodoluminescence and backscattered electron imaging to dating zircons from lower crustal xenoliths. Lithos 36:289-303
Hanchar JM, Miller CF (1993) Zircon zonation patterns as revealed by cathodoluminescence and backscattered electron images: Implications for interpretation of complex crustal histories. Chem Geol 110:1-14
Hanchar JM, Finch RJ, Hoskin PWO, Watson EB, Cherniak DJ, Mariano AN (2001) Rare earth elements in synthetic zircon: Part 1. Synthesis, and rare earth element and phosphorus doping. Am Mineral 86:667-680
He Y, Cormack AN (1999) Atomistic simulation study of defect structure of zircon as a high-level nuclear waste host form. J China Univ Geosci 10:309-313
Headley TJ, Arnold GW, Northrup CJM (1982) Dose-dependence of Pb-ion implantation damage in zirconolite, hollandite and zircon. *In* Scientific Basis for Radioactive Waste Management V. Lutze W (ed) Elsevier, p 379-388
Hinton RW, Upton BGJ (1991) The chemistry of zircon: Variations within and between large crystals from syenite and alkali basalt xenoliths. Geochim Cosmochim Acta 55: 3287-3302
Hölzl S, Hofmann AW, Todt W, Kohler H (1994) U-Pb geochronology of the Sri Lankan basement. Precambrian Res 66:23-149
Kohn MJ (1999) Why most "dry" rocks should cool "wet." Am Mineral 84:570-580
Lee JKW (1993) Problems and progress in the elucidation of U and Pb transport mechanisms in zircon. *In* Defects and Processes in the Solid State: Geocscience Applications: The McLaren Volume. Boland JN, FitzGerald JD (eds) Elsevier, p 423-446.
Lee JKW, Williams IS, Ellis DJ (1997) Pb, U and Th diffusion in natural zircon. Nature 390:159-162
Lumpkin GL, Ewing RC (1988) Alpha-decay damage in minerals of the pyrochlore group. Phys Chem Minerals 16:2-20
Magomedov SA (1970) Migration of radiogenic products in zircon (in Russian). Geokhimiya 2:263-267
Marfunin AS (1979) Spectroscopy, Luminscence, and Radiation Centers in Minerals. Springer-Verlag, Berlin, 352 p
Mariano AN (1989) Cathodoluminescence emission spectra of rare earth element activators in minerals. Rev Mineral 21:339-348
McIntyre LC Jr, Leavitt JA,Dezfouly-Arjomandy B, Oder J (1988) Depth profiling of phosphorus using resonances in the $^{31}P(\alpha,p)^{34}S$ reaction. Nucl Instr Meth B35:446-450
McLelland JM, Chiarenzelli J, Whitney P, Isachsen Y (1988) U-Pb zircon geochronology of the Adirondack Mountains and implications for their tectonic evolution. Geology 16:920-924
Medenbach O (1976) Geochemic der elemente in Zirkon und ihre Rung-Eine Untersuchung mit der elektronenstrahlmikrosonde. PhD dissertation, Ruprecht Karl Universität, 58 p
Meis C, Gale JD (1998) Computational study of tetravalent uranium and plutonium lattice diffusion in zircon. Mater Sci Engin B57:52-61
Meldrum A, Boatner LA, Weber WJ, Ewing RC (1998) Radiation damage in zircon and monazite. Geochim Cosmochim Acta 62:2509-2520
Mezger K, Krogstad EJ (1997) Interpretation of discordant U-Pb zircon ages: An evaluation. J Metamor Geol 15:127-140
Mezger K, Rawnsley C, Bohlen S, Hanson G (1991) U-Pb garnet, sphene, monazite and rutile ages: implications for the duration of high-grade metamorphism and cooling histories, Adirondack Mountains, New York. J Geol 99:415-428
Muehlenbachs K, Kushiro I (1975) Measurements of oxygen diffusion in silicates EOS Trans, Am Geophys Union 56:459
Mullen JG (1966) Theory of diffusion in ionic crystals. Phys Rev 143:658-662
Murakami T, Chakoumakos BC, Ewing RC, Lumpkin GR, Weber WJ (1991) Alpha-decay event damage in zircon. Am Mineral 76:1510-1532
Otto EM (1966) Equilibrium pressures of oxygen over oxides of lead at various temperatures. J Electrochem Soc 113:525-527
Peck WH, Valley JW, Wilde SA, Graham CM (2001) Oxygen isotope ratios and rare earth elements in 3.3 to 4.4 Ga zircons: ion microprobe evidence for high $\delta^{18}O$ continental crust and oceans in the early Archean. Geochim Cosmochim Acta 65:4215-4229
Peck WH, Valley JW, McClelland J (1999) Slow oxygen diffusion in zircon during cooling of Adirondack orthogneiss. Geol Soc Am 1999 Ann Mtg Abstr Progr 31:103
Petit JC, Dran JC, Della Mea G (1987) Effects of ion implantation on the dissolution of minerals. Part II: Selective dissolution. Bull Fr Minéral Cristallogr 110:25-42
Pidgeon RT, Nemchin AA, Hitchen GJ (1998) Internal structures of zircons from Archean granites from the Darling Range batholith: implications for zircon stability and the interpretation of zircon U-Pb ages. Contrib Mineral Petrol 132:288-299
Reeder RJ, Valley JW, Graham CM, Eiler JE (1997) Ion microprobe study of oxygen isotopic compositions of structurally nonequivalent growth surfaces on synthetic calcite. Geochim Cosmochim Acta 61:5057-5063

Reiners PW, Farley KA, Hickes HJ (2002) He diffusion and (U-Th)/He thermochronometry of zircon: initial results from Fish Canyon Tuff and Gold Butte. Tectonophysics 349:297-308
Robinson GW (1979) The occurrence of rare earth elements in zircon. PhD dissertation, Queen's University, London, Ontario, 155 p
Ryerson FJ, McKeegan KD (1994) Determination of oxygen self-diffusion in akermanite, anorthite, diopside, and spinel: implications for oxygen isotopic anomalies and the thermal histories of Ca-Al-rich inclusions. Geochim Cosmochim Acta 58:3713-3734
Sanborn N, Stern RA, Carr SD (1998) Discordance and Pb-loss mechanisms in 3.35 Ga zircon from the Acasta Gneiss complex, N.W.T., Canada: A SHRIMP ion microprobe study. Geol Soc Am Abstr Progr 30:A-240
Schärer U, Allègre CJ (1982) Uranium-lead system in fragments of a sinlge zircon grain. Nature 295:585-587
Scharer U, Corfu F, Demaiff D (1992) Heterogeneity of the subcontinental mantle: U-Pb and Lu-Hf isotopes in megacrysts of baddeleyite and zircon for the Mbuji-Mayi kimberlite. EOS Trans, Am Geophys Union Spring Mtg Suppl, p 339
Shannon RD (1976) Revised effective ionic radii and systematic studies of interatomic distances in halides and chalcogenides. Acta Crystallogr A32:751-767
Sharp ZD(1992) *In situ* laser microprobe techniques for stable isotope analysis Chem Geol 101:3-19
Shestakov GI (1969) On diffusional loss of lead from a radioactive mineral. Geochem Intl 6:888-896
Shestakov GI (1972) Diffusion of lead in monazite, zircon, sphene, and apatite. Geochem Intl 9:801-807
Shewmon P (1989) Diffusion in Solids. Minerals, Materials, and Metals Society, Warrendale, Pennsylvania
Silver LT, Deutsch S (1963) Uranium-lead isotopic variations in zircons—A case study. J Geol 71:721-758
Sinha AK, Wayne DM, Hewitt DA (1992) The hydrothermal stability of zircon: preliminary experimental and isotopic studies. Geochim Cosmochim Acta 56: 3551-3560
Smith HA, Giletti BJ (1997) Lead diffusion in monazite. Geochim Cosmochim Acta 61:1047-1055
Soltani-Farshi M, Meyer JD, Misaelides P, Bethge K (1996) Cross section of the $^{32}S(\alpha,p)^{35}Cl$ nuclear reaction for sulphur determination. Nucl Instr Meth B113: 399-402
Sommerauer J (1976) Die chemisch-physikalische Stabilität natürlicher Zirkone und ihr U-(Th)-Pb System. Doctoral dissertation, Eidgenoessischen Tech Hochschule, Zürich, Switzerland, 151 p
Speer JA (1982) Zircon. *In* Orthosilicates (2nd edn). Ribbe PH (ed) Mineral Soc Am, Rev Mineral 5:67-112
Stern RA, Sanborn N, Bleeker W (1998) Exploiting the high spatial sensitivity of the ion micoprobe in studying Pb-loss mechanisms and U-Pb ages of metamict and altered zircon. EOS Trans, Am Geophys Union, Fall Mtg Suppl, p F951
Suzuki K, Kouta H, Nagasawa H (1992) Hf-Zr interdiffusion in single crystal zircon. Geochem J 26:99-104
Valley JW, Peck WH, King EM, Wilde SA (2002) A cool early Earth. Geology 30:351-354
Valley JW, Chiarenzelli JR, McClelland JM (1994) Oxygen isotope geochemistry of zircon. Earth Planet Sci Lett 126:187-206
Valley JW, Graham CM, Harte B, Eiler JM, Kinny PD (1998) Ion microprobe analysis of oxygen, carbon, and hydrogen isotope ratios. *In* Applications of microanalytical techniques to understanding mineralizing processes. Rev Econ Geol 7:73-98
Van Orman JA, Grove TL, Shimizu N (2001) Rare earth element diffusion in diopside: Influence of temperature, pressure and ionic radius, and an elastic model for diffusion in silicates. Contrib Mineral Petrol 141:687-703
Van Orman JA, Grove TL, Shimizu N, Layne GD (2002) Rare-earth element diffusion in a natural pyrope single crystal at 2.8 GPa. Contrib Mineral Petrol 142:416-424
Vavra G, Gebauer D, Schmid R, Compston W (1996) Multiple zircon growth and recrystallization during polyphase Late Carboniferous to Triassic metamorphism in granulites of the Ivrea Zone (Southern Alps): an ion microprobe (SHRIMP) study. Contrib Mineral Petrol 122:337-358
Wang LM, Ewing RC (1992) Detailed in-situ study of ion-beam induced amorphization of zircon. Nucl Instr Meth B65:324-329
Watson EB (1980) Some experimentally determined zircon/liquid partition coefficients for the rare earth elements. Geochim Cosmochim Acta 44:895-896
Watson EB, Cherniak DJ (1997) Oxygen diffusion in zircon. Earth Planet Sci Lett 148:527-544
Watson EB, Liang Y(1995) A simple model for sector zoning in slowly grown crystals: Implications for growth rate and lattice diffusion, with emphasis on accessory minerals in crustal rocks. Am Mineral 80:1179-1187
Watson EB, Lupulescu A (1993) Aqueous fluid connectivity and chemical transport in clinopyroxene-rich rocks. Earth Planet Sci Lett 117:279-294
Watson EB, Cherniak DJ, Hanchar JM, Harrison TM, Wark DA (1997) The incorporation of Pb into zircon. Chem Geol 141:19-31
Wayne DM, Sinha AK, Hewitt DA (1992) Differential response of zircon U-Pb isotope systematics to metamorphism across a lithologic boundary: an example from the Hope Valley Shear Zone, southeastern Massachusetts, USA. Contrib Mineral Petrol 109:408-420
Weber WJ, Ewing RC, Wang LM (1994) The radiation-induced crystalline-to-amorphous transition in zircon. J

Mater Res 9:688-698
Weber WJ (1990) Radiation-induced defects and amorphization in zircon. J Mater Res 5:2687-2697
Wiechert U, Fiebig J, Przybilla R, Xiao Y, Hoefs J (2002) Excimer laser isotope-ratio-monitoring mass spectrometry for *in situ* oxygen isotope analysis Chem Geol 182:179-194
Wilde SA, Valley JW (2001) Evidence from detrital zircons for the existence of continental crust and oceans on the Earth 4.4 Gyr ago. Nature 409:175-178
Williams IS (1992) Some observations on the use of zircon U-Pb geochronology on the study of granitic rocks. Trans Royal Soc Edinburgh: Earth Sci 83:447-458
Williford RE, Weber WJ, Devanthan R, Cormak AN (1999) Native vacancy migrations in zircon. J Nucl Mater 273:164-170
Zener C (1952) Theory of diffusion. *In* Imperfections in Nearly Perfect Crystals. Shockley W, Hollomon JH, Maure R, Seitz F (eds) Wiley, New York, p 289-314
Zhang Y, Stolper EM, Wasserburg GJ (1991) Diffusion of a multi-species component and its role in oxygen and water transport in silicates. Earth Planet Sci Lett 103:228-240